COMPOSITION AND PARAGENESIS OF Pt ALLOYS FROM CHROMITITES OF THE URALIAN–ALASKAN-TYPE KYTLYM AND UKTUS COMPLEXES, NORTHERN AND CENTRAL URALS, RUSSIA

Giorgio GARUTI[§]

Dipartimento di Scienze della Terra, Universitá di Modena e Reggio Emilia, via S. Eufemia 19, I-41100 Modena, Italy

Evgeny V. PUSHKAREV

Russian Academy of Sciences, Ural Branch, Ekaterinburg, Str. Pochtovy per. 7, 620151 Ekaterinburg, Russia

Federica ZACCARINI

via B. Ramazzini 15, I-41100 Modena, Italy

ABSTRACT

Chromitites from the Kytlym and Uktus zoned Uralian–Alaskan type complexes in the northern and central Urals, Russia, contain abundant inclusions of Pt alloys compositionally attributable to one of three main groups: 1) Pt–Fe alloys with an isoferroplatinum-type composition, Pt_3Fe; 2) Ni-rich Pt–Fe–Ni–(Cu) alloys with a stoichiometry of the type isoferroplatinum $Pt_{2.5}(Fe,Ni,Cu)_{1.5}$, tetraferroplatinum $Pt(Fe,Ni,Cu)$, and ferronickelplatinum Pt_2FeNi, and 3) Cu-rich Pt–Fe–Cu–(Ni) alloys with a stoichiometry of tulameenite type, $Pt_2Fe(Cu,Ni)$. The Pt–Fe and Ni-rich Pt–Fe–Ni–(Cu) alloys occur as primary inclusions in unaltered chromian spinel and are considered to have formed in a high-temperature pre-chromite stage. A sulfide-rich assemblage (erlichmanite, Rh–Ir–Pt thiospinels, cooperite, unknown Rh–Ir-bearing base-metal sulfides, pyrrhotite and pentlandite) accompanies the Pt_3Fe alloy, indicating that it was a stable phase under relatively high sulfur fugacity. The Pt–Fe–Ni–(Cu) alloys formed at low sulfur fugacity, as suggested by the absence of sulfides and the exclusive presence of native osmium in the assemblage. The Cu-rich Pt–Fe–Cu–(Ni) alloys of tulameenite type are exclusively located along cracks in contact with secondary ferrian chromite, magnetite and chlorite, or constitute the metasomatic replacement of primary Pt alloys, and are considered to have a low-temperature hydrothermal origin. The secondary assemblage of PGM also includes potarite, prassoite, rhodian pentlandite, Cu–Pd alloys, native osmium, Ir–Fe alloys and oxides. These data strongly suggest that Ural–Alaskan-type chromitites are major contributors of Pt alloys that are encountered associated with nuggets in placer deposits of the Ural Platinum-bearing Belt.

Keywords: Pt alloys, electron-microprobe analysis, Ural–Alaskan-type chromitite, Platinum-bearing Belt, Urals, Russia.

SOMMAIRE

Les chromitites des complexes zonés de Kytlym et de Uktus, dans la partie nord et centrale des Ourales, en Russie, les deux de type dit Ourale–Alaska, contiennent une abondance d'inclusions d'alliages de Pt faisant partie d'un de trois groupes: 1) alliage Pt–Fe ayant une composition de type isoferroplatinum, Pt_3Fe; 2) alliage Pt–Fe–Ni–(Cu), enrichi en nickel, ayant une stoéchiométrie de type isoferroplatinum, $Pt_{2.5}(Fe,Ni,Cu)_{1.5}$, tétraferroplatinum, $Pt(Fe,Ni,Cu)$, ou ferronickelplatinum Pt_2FeNi, et 3) alliage Pt–Fe–Cu–(Ni), enrichi en cuivre, ayant une stoéchiométrie de type tulameenite, $Pt_2Fe(Cu,Ni)$. Les alliages Pt–Fe et Pt–Fe–Ni–(Cu) forment des inclusions primaires dans le spinelle chromifère non altéré, et auraient été formés à température élevée avant la cristallisation de la chromite. Un assemblage riche en sulfures (erlichmanite, thiospinelle à Rh–Ir–Pt, cooperite, sulfures de métaux de base contenant Rh et Ir, pyrrhotite et pentlandite) accompagne l'alliage Pt_3Fe, indication qu'il était stable à des conditions de fugacité de soufre assez élevées. L'alliage Pt–Fe–Ni–(Cu) s'est formé à une faible fugacité de soufre, comme l'indique l'absence de sulfures et la présence exclusive d'osmium natif dans l'assemblage. Les grains de l'alliage Pt–Fe–Cu–(Ni), de type tulameenite, se trouvent exclusivement le long de fissures en contact avec des minéraux secondaires comme chromite ferrique, magnétite et chlorite, ou bien remplacent les alliages platinifères primaires, et auraient donc une origine hydrothermale de basse température. Parmi les minéraux secondaires du groupe du platine se trouvent aussi potarite, prassoïte, pentlandite

---

[§] *E-mail addresses*: garutig@unimo.it, pushkarev@igg.uran.ru, fedezac@tsc4.com
This article, first printed in the April issue with defective figures, is reprinted here in its entirety.

rhodifère, alliage Cu–Pd, osmium natif, alliage Ir–Fe et oxydes. Ces données démontrent clairement que les chromitites issus de complexes de type Ourale–Alaska sont une source importante d'alliages platinifères associés aux pépites des gisements alluvionnaires de la ceinture platinifère des Ourales.

(Traduit par la Rédaction)

Mot-clés: alliages platinifères, données à la microsonde électronique, chromitite, type Ourale–Alaska, ceinture platinifère, Ourales, Russie.

INTRODUCTION

Platinum alloys are major constituents of alluvial nuggets found in a number of platinum-group-mineral (PGM) placer deposits in the world (Cabri *et al.* 1996, and references therein). In particular, they are the major carriers of Pt in placer deposits of the Urals, which were known as the major suppliers of Pt through the end of the nineteenth and the first half of the twentieth century. Shortly after the historical discovery (1819) of platinum in alluvial sediments south of Ekaterinburg, in the central Urals, several platinum placers were located in an area extending over about 900 km from the central to the northern Urals, along the 60th East meridian and between the 56° and 64° North. Because of its distinctive metallogenic signature, this province became known among Russian geologists as the "Ural Platinum-bearing Belt" (Fig. 1A). Since the end of the nineteenth century, it has been known that alluvial platinum in the Urals was mostly contributed by the erosion of upstream bodies of dunite and chromitite forming part of concentrically zoned complexes of the Uralian–Alaskan type (Fig. 1B) (Betekhtin 1961). A comparison of the relative abundance of Pt and Ir in both placer deposits of the Platinum-bearing Belt and in *in situ* mineralization within the Uralian–Alaskan-type complexes of that region established the correspondence (Razin 1976). In contrast, the Ru–Os-rich assemblages are predominantly associated with ultramafic horizons of ophiolite complexes in the Urals (Volchenko *et al.* 1995).

The mineralogy and composition of Pt alloys in alluvial nuggets from the Platinum-bearing Belt have recently been reviewed by Cabri *et al.* (1996) and Makeyev *et al.* (1997). However, comparable data for lode deposits in Uralian–Alaskan-type complexes are not available. Re-examination of Pt alloys from examples of *in situ* mineralization within chromitite and serpentinized dunite of Nizhni Tagil (Cabri & Genkin 1991, Genkin 1994) has shown that the main Pt phases are isoferroplatinum (Pt$_3$Fe) and tetraferroplatinum (PtFe), both containing minor Ir, Ni, and Cu. However, the mineral "cuproplatinum" as previously reported in the old Russian literature, has been discredited and ascribed to the species tulameenite (Pt$_2$FeCu) as defined by Cabri *et al.* (1973). Recent investigation of chromitites and dunites from the Uralian–Alaskan-type massifs of Kytlym and Uktus (Garuti *et al.* 1996, Anikina *et al.* 1999, Pushkarev *et al.* 1999) revealed that Pt alloys

with extremely variable composition are common constituents of PGM inclusions in chromian spinel. In this paper, we report the results of a systematic investigation with an electron microprobe and a scanning electron microscope of about 400 grains of Pt alloys and associated PGM. The compositional variations are directly related to the distinctive paragenetic associations in which the Pt alloys are encountered, reflecting formation at both the magmatic and the hydrothermal stages. Compositions of the Pt alloys in these lode deposits are compared with literature data concerning Pt alloys in nuggets from placers of the Ural Platinum-bearing Belt.

GEOLOGICAL SETTING

The Kytlym massif, one of the largest Ural–Alaskan-type complexes of the Platinum-bearing Belt, occurs in the Silurian island-arc of the northern Ural orogen (Fig. 1B). According to Yefimov *et al.* (1993, and references therein), the massif consists of five large blocks, dominated by distinctive rocks and associations (Fig. 1C). Gabbronorite and clinopyroxenite are major constituents of the northern (Valentorsk) and the southern (Sukhogorsk) blocks, whereas the central block (Serebryansk) mainly consists of amphibole-rich gabbro and magmatic breccia with fragments of clinopyroxenite and gabbros in a plagiogranite matrix. Dunite, clinopyroxenite, and olivine gabbro occur in the western (Konzhakov) and southwestern (Kosva Mountain) blocks, forming two sharp peaks at 1569 and 1519 meters above sea level, respectively. All blocks are characterized by a crude concentric arrangement of mineral banding, layering, and lithological contacts, typical of the Uralian–Alaskan type complexes.

FIG. 1.   A) Geological setting of the "Platinum-bearing Belt" within the Ural orogen. B) Geographical position of fifteen major Ural–Alaskan-type complexes in the Ural "Platinum-bearing Belt" (redrawn from Yefimov *et al.* 1993); 1) Revda, 2) Uktus, 3) Tagil, 4) Tagil Barancha, 5) Arbat, 6) Kachkanar, 7) Pavda, 8) Kytlym, 9) Knyaspin, 10) Kumba, 11) Denezhk, 12) Pomursk, 13) Chistop, 14) Yalping–Niersk, 15) Khorasyur. C) Geological sketch-map of the Kytlym massif, and sample location (modified after Yefimov *et al.* 1993). D) Geological sketch-map of the Uktus massif, and sample location (modified after Pushkarev *et al.* 1999).
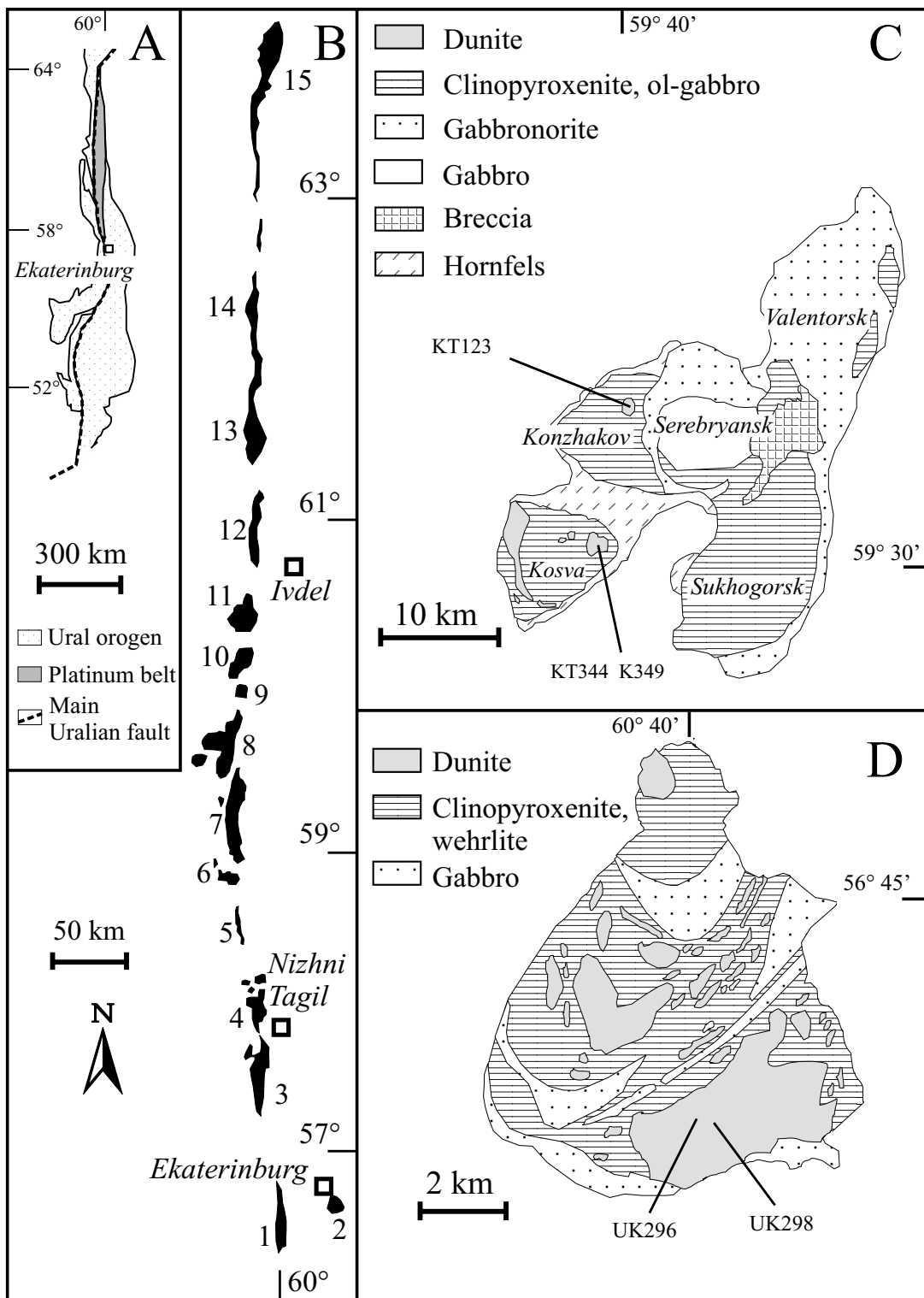
The Uktus massif, located at the southern periphery of Ekaterinburg (Fig. 1B), lies beyond the Platinum-bearing Belt, about 50 km east of the southernmost Revda complex. Despite its anomalous geological setting, the "Uralian–Alaskan" affiliation of the Uktus massif was proposed in the early 1920s, mainly on account of petrographic and structural similarities with Uralian–Alaskan type complexes *sensu stricto*. This hypothesis was petrologically supported recently (Pushkarev & Puchkova 1991, Pushkarev *et al.* 1994, Pushkarev 2000): dunite, clinopyroxenite, wehrlite, olivine gabbro and amphibole gabbro are major constituents of the rock association, and are typically arranged in a concentrically zoned structure (Fig. 1D) in which the dunites occur in a clinopyroxenite – wehrlite envelope, passing to gabbro outward.

Both the Kytlym and Uktus complexes contain subordinate chromitite occurring in close spatial association with dunite (Anikina *et al.* 1999, Pushkarev *et al.* 1999). The chromitite commonly forms pods, schlieren and veinlets, varying from a few centimeters to some decimeters across, distributed throughout the dunite hosts. Massive lenses and layers extending up to several meters in length are rare. They seem to be restricted to the southern dunite body of the Uktus complex and to dunite occurring at the core of the Konzhakov and Kosva ultramafic blocks of the Kytlym complex. Chromian spinel is typically fresh, showing only limited alteration to ferrian chromite along cracks and grain boundaries; it is associated with partially serpentinized olivine, clinopyroxene and chlorite as the major gangue silicates.

ANALYTICAL TECHNIQUES

The Pt alloys were located on polished sections by reflected-light microscopy at 250–800 × magnification, then were investigated *in situ*. Electron-microprobe analyses were performed at the Department of Earth Sciences, University of Modena and Reggio Emilia, using an ARL–SEMQ instrument equipped with both energy-dispersion and wavelength-dispersion spectrometers (EDS and WDS) and operated at an accelerating voltage of 20–27 kV and a beam current of 10–20 nA, with a beam diameter of about 1 μm. The X-ray $K\alpha$ lines were used for S, Cr, Fe, Ni, and Cu, $L\alpha$ lines for Ir, Ru, Rh, Pt, Pd, and As, and the $M\alpha$ line for Os. Pure metals were used as standards for PGE, natural chromite for Cr, and synthetic NiAs, FeS_2 and $CuFeS_2$ for Ni, Fe, Cu, S, and As. The interferences Ru–Rh, Ir–Cu, and Ru–Pd were corrected on-line. The total Fe content of the PGM included in chromite was corrected for the fluorescence effect due to the chromite according to the Cr/Fe ratio of the spinel host. Back-scattered electron (BSE) images were obtained with a Philips XL40 scanning electron microscope at the Interdepartment Instrumental Center (CIGS) of the University of Modena and Reggio Emilia.

THE PLATINUM ALLOYS

Five samples of chromitite, from a total of more than thirty investigated, were found to contain high-grade concentrations of disseminated Pt alloys, with up to 45 grains per polished section (see Figs. 1C and 1D for sample locations). The Pt alloys have compositions that plot in the Pt–Fe–Ni–Cu quaternary system. Owing to the small size of the grains, however, mostly in the range 1–35 μm, and to micro-intergrowths with other minerals, the X-ray-diffraction determinations necessary for the unequivocal identification of the mineral species (Cabri & Feather 1975) could not be carried out. For these reasons, the Pt alloys were tentatively classified on the basis of composition and considerations of stoichiometry. This approach allows identification of three different compositional groups, referred to below as: 1) Pt–Fe alloys with minor Ni and Cu, 2) Pt–Fe–Ni–(Cu) alloys containing substantial amounts of Ni and Cu, with the proportion of Ni greater than that of Cu, and 3) Pt–Fe–Cu–(Ni) alloys containing substantial amounts of Cu and Ni, with the proportion of Cu greater than that of Ni. Compositional variations in each group are plotted in the Pt–Fe–Ni–Cu tetrahedron and projected on the Pt–Fe–(Ni + Cu) triangular diagram (Fig. 2), and in three binary diagrams showing distinctive trends of Ni–Pt, Cu–Pt, and Cu–Ni reciprocal substitution in each group (Fig. 3).

The Pt–Fe alloys

The Pt alloys pertaining to the Pt–Fe group are the most abundant. More than 220 grains were identified in the chromitites of both the Kytlym (sample KT349, Kosva block) and Uktus (samples UK296, UK298) complexes. A selection of electron-microprobe results is reported in Table 1. The grains typically contain (Ni + Cu) at less than 3 at.%, which places their compositions along the Pt–Fe join of the system Pt–Fe–Ni–Cu (Fig. 2). Compositions calculated on the basis of 4 atoms per formula unit (*apfu*) cover the range from $Pt_{3.22}(Fe_{0.71}Ni_{0.05}Cu_{0.02})_{\Sigma 0.78}$ and $Pt_{2.44}(Fe_{1.47}Ni_{0.06}Cu_{0.03})_{\Sigma 1.56}$ (80.5–60.9 at.% PGE) with an average of $Pt_{2.95}(Fe_{0.99}Ni_{0.03}Cu_{0.03})_{\Sigma 1.05}$, very close to the ideal stoichiometry Pt_3Fe characteristic of the primitive cubic species *isoferroplatinum* (Cabri & Feather 1975). The extent of substitution of the other PGE for Pt is variable, reaching up to 4.2 at.% Rh, 3.7% Ir, and 1.85% Pd, whereas Ru and Os systematically do not exceed 0.5%. Very high Os contents (4.3–9.5%) observed in some analyses were ascribed to excitation of fine lamellae of native osmium observed in several grains of Pt alloy.

The Pt–Fe–Ni–(Cu) alloys

More than 100 grains of Pt–Fe alloys with Ni and Cu contents in the range 4.06–21.3 at.% and 0.93–6.04%

respectively, were analyzed from chromitite samples taken from the Kytlym complex (Table 2). Minor substitution of Rh, Ir, and Pd for Pt occurs to the same extents as in the Pt–Fe alloys. On the basis of the ratio Pt/(Fe + Ni + Cu) and the relative abundance of Ni and Cu, three different types of stoichiometries were recognized (Fig. 3).
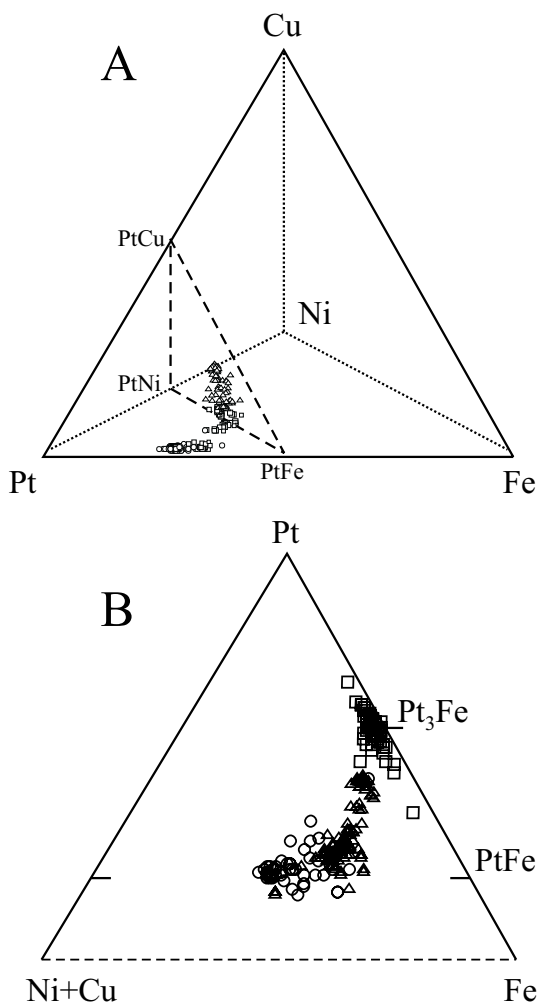
Pt$_2$FeNi type: One large grain (15 × 35 μm) in sample KT123 from the Konzhakov block was found to be unusually enriched in Ni (21.3 at.%), with relatively

FIG. 2. Plots (atom %) of compositions of the Pt alloys from chromitites of Kytlym and Uktus. A) alloys plotted in the Pt–Fe–Ni–Cu tetrahedron, showing the existence of three main groups of Pt alloys: Pt–Fe with composition close to Pt$_3$Fe (square), Pt–Fe–Ni–(Cu) varying from Pt$_{2.5}$(Fe, Ni,Cu)$_{1.5}$ to Pt(Fe,Ni,Cu) and to Pt$_2$FeNi (triangle), Pt–Fe–Cu–(Ni) alloys with composition around Pt$_2$FeCu (circle). B) Projection of the alloys onto the Pt–Fe–(Ni + Cu) diagram, showing that there is an almost continuous trend of increasing Ni and Cu with decreasing Pt:Fe ratio. The minor amounts of PGE have been added to Pt.

FIG. 3. Reciprocal variations of Ni, Cu, and Pt in the alloys from chromitites of Kytlym and Uktus. Compositions define distinctive trends for each group of Pt alloys. Pt–Fe alloys (square) are characterized by low Ni and Cu only, showing relevant variation of the Pt:Fe ratio. In Ni-rich alloys (triangle), Ni and Cu are positively correlated and progressively increase, substituting for Pt from the composition Pt$_{2.5}$(Fe,Ni,Cu)$_{1.5}$ to Pt(Fe,Ni,Cu). The Cu-rich alloys (circles) are characterized by minor variation in the Pt content, but display marked negative correlation between Ni and Cu, showing progressive substitution of Ni for Cu from tulameenite-type compositions, Pt$_2$FeCu, to tetraferroplatinum-type compositions, Pt(Fe,Ni,Cu). The minor amounts of other PGE have been added to Pt.

TABLE 1. SELECTED RESULTS OF ELECTRON-MICROPROBE ANALYSES OF
Pt–Fe ALLOYS FROM CHROMITITES, KYTLYM (KT) AND UKTUS (UK) COMPLEXES, RUSSIA

Grain No.	Os	Ir	Ru	Rh	Pt	Pd	Ni	Fe	Cu	S	As	Total
					Pt_3Fe: isoferroplatinum (?)							
KT 349B 2a 1 wt%	0.18	0.24	0.00	0.62	87.3	0.86	0.39	9.0	0.45	0.00	0.00	99.04
KT 349B 4b 4	0.16	0.54	0.07	0.26	85.3	0.92	0.29	8.3	0.42	0.00	0.00	96.26
KT 349B 5a 3	0.45	0.26	0.02	0.31	88.4	0.39	0.35	9.0	0.26	0.00	0.00	99.44
KT 349B 28b 1	5.70	0.95	0.06	0.50	80.6	0.75	0.36	8.3	0.47	0.00	0.04	97.73
KT 349C 1 2	0.17	1.99	0.00	1.11	88.0	0.36	0.19	8.8	0.18	0.00	0.06	100.86
KT 349C 5 2	0.09	0.44	0.00	0.64	88.5	0.26	0.31	8.5	0.41	0.00	0.07	99.22
KT 349C 24 1	0.24	0.39	0.08	0.07	90.4	0.14	0.27	8.5	0.13	0.00	0.00	100.22
KT 349D 19b 1	0.00	0.55	0.03	0.41	85.9	0.13	0.65	9.4	1.90	0.76	0.00	99.73
KT 349D 22a 2	0.06	3.19	0.10	0.80	87.2	0.12	0.22	8.6	0.18	0.00	0.01	100.48
UK 296A 1 1	0.23	1.49	0.00	0.79	84.9	0.00	0.28	8.5	0.36	0.00	0.02	96.57
UK 296A 12 2	0.00	0.96	0.00	0.36	88.7	0.33	0.28	8.9	0.21	0.00	0.00	99.74
UK 296B 5 1 *	0.18	1.33	0.01	0.88	84.1	0.17	0.35	8.4	0.23	0.00	0.13	95.78
UK 296B 16a 1 *	0.12	0.68	0.10	0.28	84.0	0.18	0.16	8.2	0.21	0.00	0.00	93.93
UK 298A 3c 2	0.00	1.23	0.09	0.32	92.0	0.21	0.16	8.7	0.17	0.00	0.00	102.88
UK 298A 12b 1	0.20	0.28	0.01	0.56	89.8	0.00	0.26	8.0	0.22	0.00	0.00	99.33
KT 349B 2a 1 at.%	0.14	0.19	0.00	0.95	70.1	1.27	1.03	25.2	1.12	0.00	0.00	
KT 349B 4b 4	0.14	0.45	0.12	0.42	71.3	1.40	0.80	24.3	1.07	0.00	0.00	
KT 349B 5a 3	0.38	0.21	0.04	0.48	71.3	0.59	0.94	25.4	0.66	0.00	0.00	
KT 349B 28b 1	4.81	0.80	0.10	0.79	66.3	1.14	0.98	23.8	1.19	0.00	0.09	
KT 349C 1 2	0.14	1.62	0.00	1.69	70.4	0.54	0.53	24.5	0.44	0.00	0.14	
KT 349C 5 2	0.07	0.35	0.00	0.99	72.0	0.39	0.83	24.2	1.01	0.00	0.16	
KT 349C 24 1	0.21	0.33	0.14	0.12	73.6	0.22	0.74	24.3	0.34	0.00	0.00	
KT 349D 19b 1	0.00	0.42	0.04	0.59	64.6	0.18	1.61	24.7	4.38	3.48	0.00	
KT 349D 22a 2	0.06	2.62	0.15	1.22	70.5	0.18	0.59	24.2	0.45	0.00	0.03	
UK 296A 1 1	0.19	1.26	0.00	1.24	70.7	0.00	0.76	24.9	0.91	0.00	0.04	
UK 296A 12 2	0.00	0.78	0.00	0.56	71.7	0.49	0.74	25.2	0.53	0.00	0.00	
UK 296B 5 1 *	0.16	1.13	0.02	1.41	70.6	0.26	0.98	24.6	0.59	0.00	0.25	
UK 296B 16a 1 *	0.10	0.58	0.17	0.45	72.6	0.28	0.47	24.8	0.55	0.00	0.00	
UK 298A 3c 2	0.00	0.99	0.15	0.49	73.1	0.32	0.43	24.1	0.42	0.00	0.00	
UK 298A 12b 1	0.17	0.23	0.01	0.88	74.4	0.00	0.71	23.0	0.56	0.00	0.00	

*: semiquantitative analysis.

high Cu (5.2 at.%) (anal. KT123–1, Table 2). The composition calculated on the basis of 4 apfu corresponds to $Pt_{1.98}(Fe_{0.99}Ni_{0.82}Cu_{0.20})_{\Sigma 2.02}$, consistent with the tetragonal species *ferronickelplatinum* (ideal Pt_2FeNi, after Rudashevskii et al. 1983), with some Cu substituting for Ni.

Pt(Fe,Ni,Cu) type: A large number of the grains of Pt–Fe–Ni–(Cu) alloy were found in sample KT344 from the Kosva block. These grains have an average composition expressed by the formula $Pt_{1.07}(Fe_{0.61}Ni_{0.22}Cu_{0.1})_{\Sigma 0.93}$ on 2 apfu, with significant amounts of Ni (9.05–12.9 at.%) and Cu (2.39–6.04 at.%). This mineral is probably analogous to compositions previously described in the literature (Cabri et al. 1977, Nixon et al. 1990) and interpreted as a Ni-rich variety of the tetragonal alloy *tetraferroplatinum* (Cabri & Feather 1975), although the Pt content is usually in slight excess compared with the ideal stoichiometry PtFe.

Pt2.5(Fe,Ni,Cu)1.5 type: A Pt–Fe–Ni–(Cu) alloy characterized by a relatively low proportion of Ni (4.06–7.35 at.%) and Cu (0.93–1.63 at.%) also occurs in sample KT344. The average composition calculated on the basis of 4 atoms gave $Pt_{2.62}(Fe_{1.11}Ni_{0.22}Cu_{0.05})_{\Sigma 1.38}$, very similar to the alloy $Pt_{2.5}(Fe,Ni,Cu)_{\Sigma 1.5}$ reported from Tulameen and tentatively ascribed to *isoferroplatinum* (Nixon et al. 1990). We note, however, that the phase is Pt-deficient and relatively enriched in Ni and Cu compared with the isoferroplatinum generally encountered at Kytlym and Uktus. In addition, the same composition recalculated on the basis of 3 apfu results in the formula $Pt_{1.96}(Fe_{0.83}Ni_{0.17}Cu_{0.04})_{\Sigma 1.04}$, closely resembling the stoichiometry $Pt_2(Fe,Ni,Cu)$ that has been frequently reported as unnamed Pt_2Fe in nature (Daltry & Wilson 1997), possibly representing a phase distinct from isoferroplatinum.

Several grains of Pt–Fe–Ni–(Cu) alloy have a composition intermediate between the two last types. It is possible that some of these compositions have resulted from analysis of a mixture of Ni-rich varieties of isoferroplatinum and tetraferroplatinum, since the two phases were locally found to coexist within a single grain (i.e., see below, Figs. 7A, B). However, relatively large grains that have such an intermediate stoichiometry [$Pt_{2.25}(Fe_{1.20}Ni_{0.38}Cu_{0.18})_{\Sigma 1.75}$] proved to be homogeneous under SEM examination, indicating that they likely represent true compositions. If this is the case, a

clear trend of sympathetic increase in Ni and Cu, both substituting for Pt (Fig. 3), occurs from $Pt_{2.5}(Fe,Ni,Cu)_{1.5}$ to $Pt(Fe,Ni,Cu)$, suggesting the possible existence of solid solution in the group of Pt–Fe–Ni–(Cu) alloys.

The Pt–Fe–Cu–(Ni) alloys

More than 50 grains from Kytlym (sample KT349, Kosva block) and Uktus (samples UK296, UK298) are

TABLE 2. SELECTED RESULTS OF ELECTRON-MICROPROBE ANALYSES OF
Pt–Fe–Ni–(Cu) ALLOYS FROM CHROMITITES, KYTLYM (KT) AND UKTUS (UK) COMPLEXES, RUSSIA

Grain No.	Os	Ir	Ru	Rh	Pt	Pd	Ni	Fe	Cu	S	As	Total
$Pt_{2.5}(Fe,Ni,Cu)_{1.5}$: isoferroplatinum (?)												
KT 344A 29b 1 wt%	0.00	0.96	0.08	1.06	83.7	0.33	2.20	10.6	0.47	0.00	0.00	99.40
KT 344B 14 1	0.11	1.57	0.10	1.16	80.7	0.40	2.99	11.5	0.91	0.00	0.00	99.44
KT 344B 9b 1	0.06	1.33	0.06	1.44	82.5	0.25	2.94	11.6	0.89	0.00	0.00	101.07
KT 344C 12 1	0.21	1.25	0.04	0.96	82.5	0.55	2.26	10.5	0.57	0.00	0.00	98.84
KT 344C 3 1	0.00	1.45	0.05	0.81	82.2	0.53	1.90	10.7	0.70	0.00	0.00	98.34
KT 344D 12 1 *	0.11	0.87	0.04	1.29	83.1	0.33	2.98	12.0	1.09	0.00	0.00	101.81
$Pt(Fe,Ni,Cu)$: tetraferroplatinum (?)												
KT 344A 18a 1	0.46	1.20	0.06	0.89	78.4	0.37	3.95	12.5	1.61	0.00	0.00	99.44
KT 344A 21 1	0.14	0.90	0.08	1.10	77.9	0.21	4.16	12.3	1.72	0.00	0.00	98.51
KT 344A 27 1	0.00	0.90	0.07	0.93	78.3	0.32	3.91	12.1	1.70	0.00	0.00	98.23
KT 344B 17 1	0.10	0.61	0.04	1.43	76.3	0.21	4.75	12.3	2.25	0.00	0.15	98.14
KT 344B 18 1	0.08	1.33	0.04	1.06	75.9	0.28	5.14	12.2	2.18	0.00	0.03	98.24
KT 344B 22 1	0.03	1.23	0.00	1.29	77.8	0.22	4.39	12.6	1.91	0.00	0.00	99.47
KT 344B 28 1	0.32	1.27	0.00	0.70	76.7	0.40	4.36	12.4	1.97	0.00	0.00	98.12
KT 344C 19 1	0.22	4.49	0.12	1.31	72.4	0.25	4.43	13.4	2.07	0.00	0.00	98.69
KT 344D 1a 1	0.03	1.02	0.06	1.05	77.7	0.29	4.07	13.4	2.13	0.00	0.03	99.78
KT 344D 11 1	0.06	0.80	0.06	1.59	77.8	0.27	4.02	12.8	2.18	0.00	0.11	99.69
KT 344D 12 9 *	0.00	0.47	0.05	0.96	76.4	0.29	3.79	14.1	1.96	0.00	0.00	98.02
KT 344D 20 1	0.10	0.64	0.01	1.10	78.1	0.21	4.45	13.3	2.37	0.00	0.05	100.33
Pt_2FeNi: ferronickelplatinum												
KT 123 1	0.00	5.92	0.16	0.44	69.7	0.00	10.3	11.4	2.56	0.00	0.03	100.51
KT 123 2	0.04	5.09	0.09	0.27	70.3	0.00	10.1	11.3	2.66	0.00	0.00	99.85
KT 123 3	0.30	4.55	0.00	0.30	70.8	0.05	9.95	11.2	2.84	0.00	0.05	100.04
$Pt_{2.5}(Fe,Ni,Cu)_{1.5}$: isoferroplatinum (?)												
KT 344A 29b 1 at.%	0.00	0.72	0.11	1.50	62.8	0.44	5.47	27.9	1.06	0.00	0.00	
KT 344B 14 1	0.08	1.15	0.14	1.59	58.3	0.53	7.19	29.0	2.02	0.00	0.00	
KT 344B 9b 1	0.05	0.96	0.09	1.95	58.8	0.33	6.96	28.9	1.96	0.00	0.00	
KT 344C 12 1	0.15	0.95	0.06	1.36	62.2	0.75	5.63	27.6	1.30	0.00	0.00	
KT 344C 3 1	0.00	1.11	0.07	1.17	62.3	0.73	4.78	28.2	1.64	0.00	0.00	
KT 344D 12 1 *	0.08	0.62	0.06	1.72	58.4	0.43	6.94	29.4	2.35	0.00	0.00	
$Pt(Fe,Ni,Cu)$: tetraferroplatinum (?)												
KT 344A 18a 1	0.33	0.84	0.08	1.16	54.4	0.47	9.09	30.2	3.43	0.00	0.00	
KT 344A 21 1	0.10	0.64	0.11	1.46	54.3	0.26	9.64	29.8	3.69	0.00	0.00	
KT 344A 27 1	0.00	0.64	0.10	1.23	55.1	0.42	9.13	29.7	3.68	0.00	0.00	
KT 344B 17 1	0.07	0.43	0.05	1.86	52.2	0.28	10.8	29.3	4.75	0.00	0.26	
KT 344B 18 1	0.06	0.92	0.05	1.38	51.9	0.35	11.7	29.0	4.59	0.00	0.05	
KT 344B 22 1	0.02	0.85	0.00	1.69	53.1	0.27	9.96	30.1	4.01	0.00	0.00	
KT 344B 28 1	0.23	0.90	0.00	0.94	53.2	0.52	10.0	30.0	4.21	0.00	0.00	
KT 344C 19 1	0.15	3.07	0.15	1.68	48.8	0.31	9.94	31.6	4.30	0.00	0.00	
KT 344D 1a 1	0.02	0.70	0.08	1.35	52.4	0.35	9.13	31.5	4.41	0.00	0.06	
KT 344D 11 1	0.04	0.54	0.08	2.02	52.9	0.33	9.07	30.3	4.53	0.00	0.19	
KT 344D 12 9 *	0.00	0.33	0.07	1.22	51.9	0.35	8.54	33.5	4.09	0.00	0.00	
KT 344D 20 1	0.07	0.42	0.02	1.37	51.8	0.25	9.79	31.4	4.80	0.00	0.08	
Pt_2FeNi: ferronickelplatinum												
KT 123 1	0.00	3.78	0.19	0.53	43.8	0.00	21.6	25.1	4.95	0.00	0.05	
KT 123 2	0.02	3.27	0.10	0.31	44.7	0.00	21.3	25.1	5.18	0.00	0.00	
KT 123 3	0.20	2.95	0.00	0.37	45.0	0.05	21.0	24.8	5.55	0.00	0.08	

*: compositions coexisting in grain KT 344D 12 (Fig. 7A).

ascribed to the Pt–Fe–Cu–(Ni) group of Pt alloys (Table 3). The group as a whole is characterized by a rather constant stoichiometry $Pt_2Fe(Cu>Ni)$, with minor substitution of Pd, Rh, and Ir for Pt. The most Cu-rich compositions correspond to the average formula $Pt_{2.06}Fe_{0.96}(Cu_{0.89}Ni_{0.09})_{\Sigma0.98}$, calculated on the basis of 4 *apfu*, similar to that of tetragonal tulameenite (ideal Pt_2FeCu after Cabri *et al.* 1973). Contrary to the Ni-rich varieties of Pt alloys described above, there is a progressive increase in Ni at the expense of Cu (Fig. 3) up to the field of (Ni + Cu)-rich tetraferroplatinum, showing some compositional overlap between these phases. In fact, some calculated stoichiometries, for example $Pt_{2.04}Fe_{1.00}(Cu_{0.54}Ni_{0.42})_{\Sigma0.96}$, may be regarded either as Ni-rich tulameenite or as Cu-rich tetraferroplatinum. Some grains of Pt–Fe–Cu–(Ni) alloy seem to be heterogeneous in composition, with a wide variation in Cu:Ni ratio within a single grain, although the association does not appear to be due to subsolidus unmixing, the texture being more consistent with replacement (see below).

MORPHOLOGY, TEXTURE AND PARAGENETIC ASSEMBLAGES

Morphology, texture and paragenetic assemblages of the Pt alloys provide constraints on their order of crystallization with respect to the mineral constituting the host chromitite, and information on the chemical and physical conditions prevailing at the time of their precipitation. On this basis, we have recognized different assemblages of Pt alloys: "primary", having crystallized at high temperature as part of the chromite precipitation event, and "secondary", having formed as result of remobilization of PGE due to hydrothermal events.

Primary assemblages of Pt alloys

The Pt alloys in the primary category are pure isoferroplatinum (Pt_3Fe), and the Ni-rich varieties corresponding to isoferroplatinum $Pt_{2.5}(Fe,Ni,Cu)_{1.5}$, tetraferroplatinum $Pt(Fe,Ni,Cu)$, and ferronickelplati-

TABLE 3. SELECTED RESULTS OF ELECTRON-MICROPROBE ANALYSES OF
Pt–Fe–Cu–(Ni) ALLOYS FROM CHROMITITES, KYTLYM (KT) AND UKTUS (UK) COMPLEXES, RUSSIA

Grain No.	Os	Ir	Ru	Rh	Pt	Pd	Ni	Fe	Cu	S	As	Total
Pt_2FeCu: tulameenite												
KT 349A 6 1 wt%	0.05	0.00	0.03	0.44	77.9	0.15	1.16	9.95	11.1	0.00	0.05	100.83
KT 349B 34a 1	0.00	0.16	0.06	0.71	77.5	0.00	0.66	10.6	11.4	0.00	0.00	101.09
KT 349B 36a 4	0.20	0.29	0.09	0.60	76.1	0.71	0.46	13.5	8.04	0.00	0.04	100.03
KT 349C 13 4	0.20	0.41	0.19	0.47	76.7	0.10	0.75	10.0	12.2	0.00	0.01	101.03
KT 349C 22 1	0.21	0.00	0.25	0.36	76.1	0.04	3.05	12.5	6.66	0.00	0.00	99.17
KT 349D 27b 1	0.00	0.33	0.01	0.58	76.3	0.44	3.26	10.3	9.07	0.00	0.01	100.30
KT 349D 33a 1	0.22	0.15	0.04	0.34	77.5	0.00	2.50	11.0	8.22	0.00	0.02	99.99
KT 349D 8b 1	0.24	0.25	0.00	0.76	75.1	0.11	2.75	11.1	9.33	0.00	0.00	99.64
UK 296B 9 3	0.00	1.97	0.08	0.94	75.8	0.00	2.05	9.34	7.29	0.00	0.00	97.47
UK 296A 9 2	0.00	0.38	0.06	0.15	73.8	0.06	1.44	11.9	9.27	0.00	0.00	97.06
UK 298A 3c 8	0.21	0.77	0.00	0.73	77.0	0.00	0.35	10.5	10.7	0.00	0.00	100.26
UK 298B 14a 1	0.17	0.23	0.00	0.24	77.2	0.00	1.86	10.0	9.07	0.00	0.01	98.78
KT 349D 21a 1	0.09	0.30	0.21	0.78	76.1	0.11	3.53	10.5	7.00	0.00	0.07	98.69
KT 349B 37a 2	0.00	0.21	0.03	0.36	76.1	0.04	0.81	9.76	12.3	0.00	0.08	99.69
KT 349B 37b 1	0.00	0.33	0.07	0.65	75.3	1.73	3.98	11.5	5.12	0.00	0.00	98.68
KT 344C 11 1	0.08	1.03	0.00	1.05	74.6	0.00	3.53	10.8	7.35	0.00	0.00	98.45
Pt_2FeCu: tulameenite												
KT 349A 6 1 at.%	0.03	0.00	0.03	0.55	51.2	0.18	2.52	22.9	22.5	0.00	0.09	
KT 349B 34a 1	0.00	0.11	0.08	0.88	50.6	0.00	1.43	24.2	22.7	0.00	0.00	
KT 349B 36a 4	0.13	0.19	0.12	0.74	49.9	0.85	1.00	30.8	16.2	0.00	0.07	
KT 349C 13 4	0.13	0.28	0.23	0.59	50.0	0.12	1.64	22.7	24.3	0.00	0.01	
KT 349C 22 1	0.14	0.00	0.31	0.44	50.1	0.05	6.66	28.8	13.5	0.00	0.00	
KT 349D 27b 1	0.00	0.22	0.01	0.73	49.8	0.53	7.09	23.4	18.2	0.00	0.02	
KT 349D 33a 1	0.15	0.10	0.04	0.43	51.4	0.00	5.54	25.5	16.8	0.00	0.04	
KT 349D 8b 1	0.16	0.17	0.00	0.96	48.9	0.13	5.98	25.1	18.6	0.00	0.00	
UK 296B 9 3	0.00	1.41	0.11	1.26	53.6	0.00	4.82	23.0	15.8	0.00	0.00	
UK 296A 9 2	0.00	0.26	0.08	0.18	49.3	0.07	3.21	27.8	19.1	0.00	0.00	
UK 298A 3c 8	0.15	0.53	0.00	0.93	51.3	0.00	0.79	24.5	21.8	0.00	0.00	
UK 298B 14a 1	0.12	0.16	0.00	0.30	52.5	0.00	4.20	23.8	18.9	0.00	0.02	
KT 349D 21a 1	0.06	0.20	0.27	1.01	51.2	0.14	7.90	24.6	14.5	0.00	0.12	
KT 349B 37a 2	0.00	0.14	0.04	0.45	50.1	0.05	1.79	22.5	24.8	0.00	0.13	
KT 349B 37b 1	0.00	0.22	0.10	0.81	50.5	2.12	8.85	26.8	10.6	0.00	0.00	
KT 344C 11 1	0.06	0.69	0.00	1.31	49.9	0.00	7.84	25.1	15.1	0.00	0.00	

num Pt_2FeNi. They typically are euhedral to subhedral, and occur as minute crystals locked in fresh chromian spinel, far from fractures and zones of alteration. These alloys are found in three separate chromitite samples characterized by distinctive assemblages of primary PGM inclusions.

Pure isoferroplatinum (Pt_3Fe) with rare exsolution lamellae of osmium invariably is found in a sulfur-rich assemblage of PGM (erlichmanite, PGE-thiospinels, cooperite) and base metals (pyrrhotite, pentlandite and an unknown Rh–Ir–Pt–Fe–Ni–Cu sulfide) (samples KT349, UK296, UK298). Analytical results for these minerals are reported in Table 4. Compositions of erlichmanite and PGE-thiospinels are shown in Figures 4A and 4B, respectively. Erlichmanite ranges in composition between $[Os_{0.89}Ru_{0.01}(Ir,Rh,Pt)_{\Sigma 0.1}]S_2$ and

$[Os_{0.48}Ru_{0.35}(Ir,Rh,Pt)_{\Sigma 0.17}]S_2$, whereas the thiospinels show a wide range of Rh–Ir–Pt incorporation: Ir- and Pt-rich cuprorhodsite $(Rh_{0.82}Ir_{0.47}Pt_{0.68})_{\Sigma 1.97}(Cu_{0.74}Fe_{0.27})_{\Sigma 1.01}S_{4.02}$, Rh- and Pt-rich cuproiridsite $(Ir_{0.89}Rh_{0.88}Pt_{0.30})_{\Sigma 2.07}(Cu_{0.63}Fe_{0.28})_{\Sigma 0.91}S_{4.02}$, and Rh- and Ir-rich malanite $(Pt_{0.92}Rh_{0.63}Ir_{0.48})_{\Sigma 2.03}(Cu_{0.92}Fe_{0.03})_{\Sigma 0.95}S_{4.02}$. The unknown Rh–Ir–Pt–Fe–Ni–Cu sulfide has Fe and Rh as the major constituents, accompanied by minor Os, Ir, Pt, Ni, and Cu. Compositions are consistent with a monosulfide stoichiometry of the type $(Fe,Ni,Cu)_2(Rh,Ir,Pt)S_3$, suggesting that the phase may represent a PGE-rich variety of pyrrhotite or pentlandite (Cabri *et al.* 1981, Garuti *et al.* 1995). Cooperite has a constant composition close to $(Pt_{0.98}Pd_{0.02}Rh_{0.01}Ni_{0.02})_{\Sigma 1.03}S_{0.97}$.

Several grains from both Uktus (Fig. 5) and Kytlym (Fig. 6) display textural evidence indicating that the sulfide erlichmanite grew over pre-existing crystals of isoferroplatinum prior to entrapment into chromite. In other cases, isoferroplatinum is overgrown by a complex assemblage consisting of erlichmanite, PGE-thiospinels, an unknown Rh–Ir–Pt–Fe– Ni–Cu sulfide, pentlandite and pyrrhotite. Cooperite was found exclusively as free grains independent of Pt alloys.

In contrast with Pt_3Fe, the Ni-rich varieties isoferroplatinum $Pt_{2.5}(Fe,Ni,Cu)_{\Sigma 1.5}$ and tetraferroplatinum $Pt(Fe,Ni,Cu)$ occur in a PGM assemblage characterized by the absence of sulfides (sample KT344). The most common accessory PGM is native osmium, which generally occurs either associated with the Pt alloys (Fig. 7) or as free euhedral crystals included in chromian spinel. Osmium has a rather homogeneous composition (Table 4), with low levels of Ir (1.3–8.8 at.%) and Pt (0.0–9.4 at.%), whereas Ru, Rh, Ni and Fe are usually lower than 1.0 at.% and Pd occurs in trace amounts (Fig. 4A). As mentioned in the composition section, the Ni-rich tetraferroplatinum $Pt_{2.16}(Fe_{1.34}Ni_{0.34}Cu_{0.16})_{\Sigma 1.84}$ and isoferroplatinum $Pt_{2.54}(Fe_{1.2}Ni_{0.21}Cu_{0.05})_{\Sigma 1.46}$ occur in single grains together with native osmium (Figs. 7A, B). The association is similar to that described by Nixon *et al.* (1990) at Tulameen, although in the present case the internal textures of the grains do not support the hypothesis that isoferroplatinum (Pt_3Fe) originated by diffusion of Fe from tetraferroplatinum (PtFe) to the host chromite. The association can reasonably be explained by subsolidus exsolution reactions, starting from an initially homogeneous alloy phase.

Like Ni-rich tetraferroplatinum and isoferroplatinum, the ferronickelplatinum occurs in composite inclusions with osmium and in the apparent absence of PGM sulfides (sample KT123). Abundant Ni sulfides (heazlewoodite and millerite) occur in the same sample, although their exclusive association with serpentine-filled cracks in the chromian spinel indicate that they are part of the secondary assemblage produced during low-temperature alteration of the chromitites.

FIG. 4. A) Compositions (atom %) of Os–Ir–Ru sulfides (open circles) and alloys (full circles) coexisting with primary Pt alloys from chromitites of Kytlym and Uktus. B) Compositions of Rh–Ir–Pt thiospinels found in primary composite grains with isoferroplatinum-type alloys (Pt_3Fe). See text for explanation.

Secondary Pt alloys and replacement associations

Significantly, the Pt–Fe–Cu–(Ni) alloys with tulameenite-type stoichiometry were never found completely encapsulated in unfractured chromian spinel, as is typical of primary Pt alloys. They were observed in all samples except KT123, commonly forming large discrete grains located in interstitial patches of chlorite and along cracks cutting across chromian spinel, or appearing to partially replace primary magmatic Pt alloys that are locally in contact with fractures. Their textural relationships and paragenetic assemblages indicate that the Pt–Fe–Cu–(Ni) alloys formed at a late stage after fracturing of chromian spinel, possibly by direct deposition from hydrothermal solutions producing the chlorite and the ferrian chromite alteration.

Examples of free grains of secondary Pt–Fe–Cu–(Ni) alloys are shown in Figures 8 and 9. One large tabular crystal of almost pure tulameenite, $Pt_{2.08}Fe_{0.94}(Ni_{0.05}$

$Cu_{0.93})_{\Sigma 0.98}$, containing minute inclusions of irarsite and Ni-rich tetraferroplatinum, was observed in interstitial chlorite (Figs. 8A, B), close to an elongate aggregate of rhodian pentlandite and heazlewoodite that hosts a small grain of an unknown Cu–Pd alloy. A continuous rim of ferrian chromite separates the chlorite from the fresh chromian spinel, and both chlorite and ferrian chromite are finely veined with Pd Hg (potarite?), indicating the presence of a circulating PGE-bearing hydrothermal fluid. Tulameenite seems to occur in the chlorite-filled cracks in spatial association with late magnetite (Mgt). It contains lamellae of an Fe-oxide, supporting a secondary origin for the tulameenite with respect to the crystallization of chromian spinel (Fig. 8C). Some grains of tulameenite located in fractured chromite are remarkably porous and show concentric compositional zoning. As an example, the grain (Fig. 8D) associated with chlorite in altered chromite consists of a colloform aggregate of alternating shells of tulameenite and an
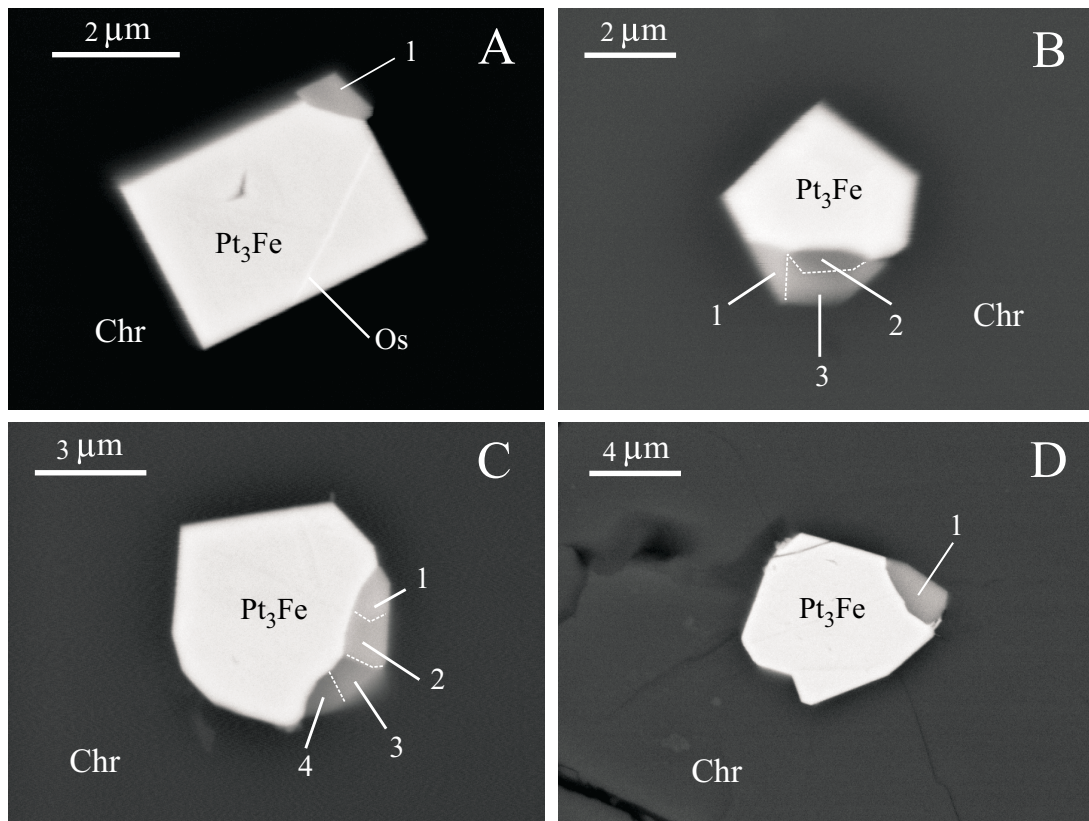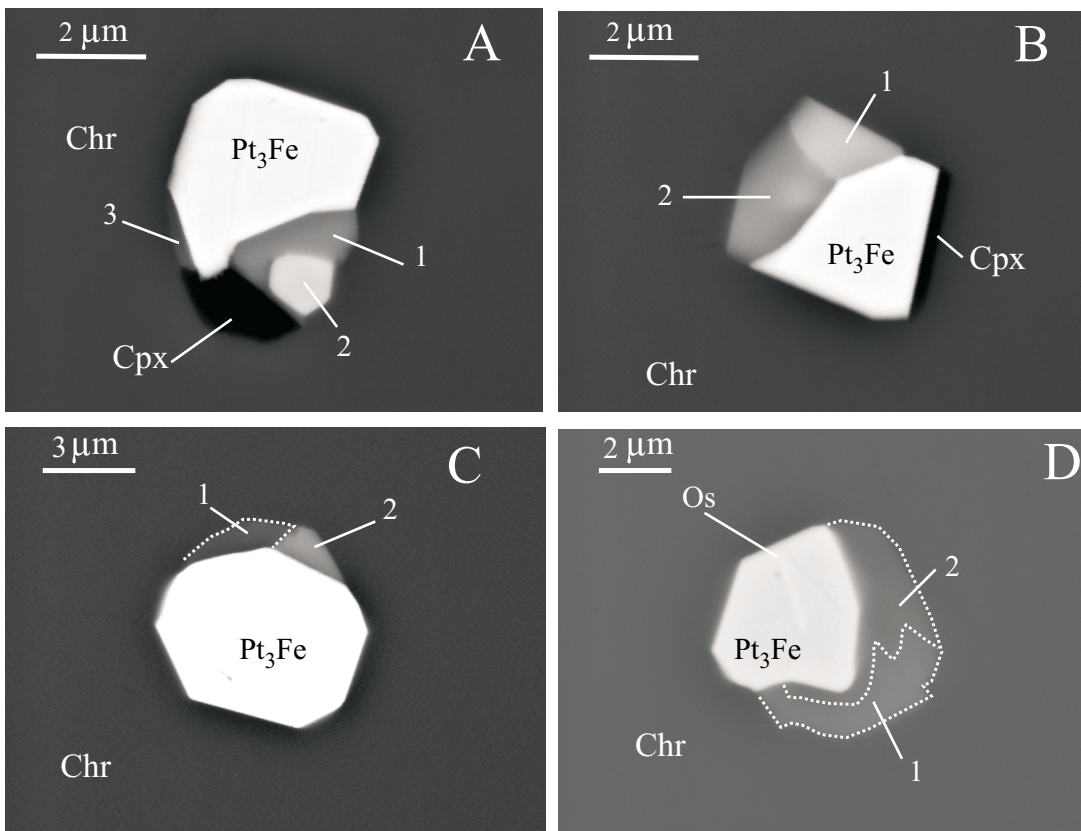

FIG. 5. BSE images of primary composite grains included in chromian spinel (Chr) from the Uktus chromitites, showing isoferroplatinum-type alloys (Pt_3Fe) overgrown by PGE sulfides. A) Grain UK296B–5, erlichmanite (1). Isoferroplatinum contains one thin exsolution lamella of native osmium (Os). B) Grain UK296B–16a, erlichmanite (1), cuprorhodsite (2) and cuproiridsite (3). C) Grain UK296A–1, erlichmanite (1), Ru-rich erlichmanite (2), cuproiridsite (3), and cuprorhodsite (4). D) Grain UK296A–12, cuprorhodsite $(Cu_{0.72}Ni_{0.08}Fe_{0.04})_{\Sigma 0.84}(Rh_{1.24}Ir_{0.81}Pt_{0.02})_{\Sigma 2.08}S_{4.08}$.

FIG. 6. BSE images of primary composite grains included in chromian spinel (Chr) from the Kytlym chromitites, showing isoferroplatinum-type alloys (Pt$_3$Fe) overgrown by various sulfides and clinopyroxene (not ubiquitous). A) Grain KT349B–2a, unknown PGE-bearing base-metal monosulfide (Fe$_{0.27}$Ni$_{0.22}$Cu$_{0.08}$)$_{\Sigma0.57}$(Rh$_{0.17}$Ir$_{0.08}$Os$_{0.08}$Pt$_{0.04}$)$_{\Sigma0.37}$S$_{1.06}$ (1), erlichmanite (Os$_{0.68}$Ir$_{0.04}$Ru$_{0.13}$Ni$_{0.09}$Fe$_{0.02}$)$_{\Sigma0.96}$S$_{2.04}$ (2), Fe–Ni sulfide, possibly pentlandite (3), and clinopyroxene (Cpx). B) Grain KT349B–4b, cuprorhodsite (Cu$_{0.73}$Fe$_{0.27}$Ni$_{0.06}$)$_{\Sigma1.06}$(Rh$_{0.75}$Ir$_{0.47}$Pt$_{0.68}$Os$_{0.07}$Ru$_{0.02}$)$_{\Sigma1.99}$S$_{3.95}$ (1), unknown PGE-bearing base-metal monosulfide (Fe$_{0.27}$Ni$_{0.17}$Cu$_{0.12}$)$_{\Sigma0.56}$(Rh$_{0.19}$Ir$_{0.1}$Os$_{0.05}$Pt$_{0.02}$Pd$_{0.02}$)$_{\Sigma0.38}$S$_{1.06}$ (2), and clinopyroxene (Cpx). C) Grain KT349B–5a, pyrrhotite Fe$_{0.96}$Ni$_{0.02}$(Rh + Pt)$_{0.02}$S$_{1.0}$ (1), and unknown PGE-bearing base-metal monosulfide (Fe$_{0.27}$Ni$_{0.23}$Cu$_{0.12}$)$_{\Sigma0.62}$(Rh$_{0.23}$Ir$_{0.05}$Pt$_{0.06}$)$_{\Sigma0.34}$S$_{1.04}$ (2). D) Grain KT349B–28b, pentlandite (1), and pyrrhotite (2). The grain contains one exsolution lamella of native osmium (Os).

unidentified Cu-rich Pt alloy. Interpretation of this texture suggests sequential growth of the concentric bands from pulses of hydrothermal fluids. Late precipitation of Cu-rich Pt alloy from circulating fluids is also supported by the finding of such alloy in microscopic fractures in fresh chromite (Fig. 9A). The fracture is in physical continuity with a composite inclusion mainly consisting of tulameenite, native Cu and rhodian pentlandite, whereas small particles of erlichmanite and Pt–Fe alloy occur within the tulameenite (Fig. 9B). Interpretation of this assemblage is problematic, as it occurs in fresh chromian spinel. However, the porous aspect of tulameenite and native Cu, as well as the presence of a Pt–Fe alloy and erlichmanite, suggest an origin by late replacement of a primary inclusion of isoferroplatinum plus sulfides, by reaction with a Cu–Pt-rich fluid that traveled through the fissure.

Several associations of replacement minerals were observed at Uktus. One zoned inclusion located in a fracture (Fig. 9C) represents a primary grain of isoferroplatinum, with a relict polygonal shape, in contact with fresh chromian spinel. It is replaced along the contact with ferrian chromite by Ni-rich tulameenite of extremely heterogeneous composition. The largest grain studied during this investigation (Fig. 10, UK298A–3c) consists of tulameenite, isoferroplatinum, erlichmanite, and a spongy polyphase aggregate of Ni-rich tulameenite, an unknown Rh sulfide with a composition close to

TABLE 4. SELECTED RESULTS OF ELECTRON-MICROPROBE ANALYSES OF
PGM ASSOCIATED WITH Pt ALLOYS FROM CHROMITITES,
KYTLYM (KT) AND UKTUS (UK) COMPLEXES, RUSSIA

Grain No.	Os	Ir	Ru	Rh	Pt	Pd	Ni	Fe	Cu	S	As	Total
Osmium												
KT 344C 34 1 wt%	90.1	3.58	0.36	0.19	5.43	0.09	0.59	0.21	0.00	0.00	0.00	100.55
KT 344D 12 3	98.2	1.63	0.33	0.26	3.17	0.05	0.17	0.30	0.00	0.00	0.00	104.11
KT 344D 1b 1	93.6	5.98	0.36	0.01	0.77	0.03	0.11	0.04	0.00	0.00	0.01	100.91
KT 344D 20 2	97.7	2.26	0.23	0.00	0.25	0.02	0.10	0.08	0.00	0.00	0.12	100.76
KT 344D 4a 1	87.0	6.24	0.40	0.44	2.98	0.07	0.19	0.29	0.00	0.00	0.05	97.66
KT344D 12 10	86.3	5.14	0.31	0.24	4.18	0.05	0.28	1.22	0.00	0.00	0.01	97.73
UK 296A 5b 2	96.9	1.29	0.18	0.13	2.00	0.00	0.04	0.02	0.00	0.00	0.01	100.57
Erlichmanite												
KT 349B 36a 3	63.5	4.72	4.59	0.71	0.41	0.12	0.08	0.12	0.03	25.5	0.11	99.89
KT 349C 13 2	54.8	4.69	7.11	1.89	0.00	0.36	0.03	0.34	0.09	27.8	0.00	97.11
KT 349C 13 3	52.0	5.86	9.13	2.01	0.00	0.32	0.14	0.40	0.24	27.7	0.00	97.80
UK 298A 3c 3	67.7	5.66	0.51	1.29	0.00	0.00	0.03	0.08	0.00	25.3	0.00	100.57
Cooperite												
KT 349B 45b 1	0.01	0.54	0.10	0.78	82.5	0.77	0.70	0.00	0.00	13.2	0.00	98.60
KT349A 13a 1	0.02	0.00	0.00	0.27	83.8	0.81	0.57	0.00	0.00	13.3	0.00	98.77
UK 298A 6 1	7.55	0.68	1.33	0.67	72.3	0.21	0.30	0.35	0.44	14.1	0.00	97.93
UK 298B 5 2	0.04	0.26	0.00	0.61	84.9	0.36	0.46	0.00	0.00	13.0	0.00	99.63
Rh–Ir–Pt thiospinels												
KT 349B 12a 2	1.33	16.5	0.00	28.3	8.56	2.09	3.51	6.02	6.77	24.0	0.00	97.11
KT 349B 2c 1	0.00	17.2	0.00	31.3	10.1	0.00	0.18	4.10	10.3	25.8	0.00	98.95
KT 349B 4b 3 *	2.45	16.7	0.43	14.4	24.5	0.20	0.69	2.80	8.64	23.8	0.00	94.66
KT 349C 5 3	2.10	31.7	0.08	17.1	11.0	0.70	0.06	2.96	7.38	24.1	0.07	97.19
KT 349A 16 4	2.65	15.2	0.17	28.3	15.0	0.00	0.10	5.20	4.91	24.3	0.01	95.76
UK 296A 12 1	0.21	32.2	0.00	26.3	0.92	0.00	0.98	0.48	9.36	26.9	0.04	97.42
UK 296A 3 1	0.00	17.4	0.00	12.2	33.5	0.00	0.04	0.31	10.8	24.1	0.00	98.33
UK 296A 3 2	0.00	16.7	0.00	12.3	33.0	0.42	0.00	0.34	10.8	23.3	0.02	96.85
UK 296A 4 1 *	0.07	19.5	0.00	10.1	32.8	0.00	0.11	0.06	10.2	23.1	0.00	95.90
unknown Rh–Ir sulfides												
KT 349B 2a 3	11.9	12.4	0.63	13.3	6.61	0.00	9.76	11.9	4.04	26.3	0.02	96.83
KT 349B 4b 1	8.49	15.0	0.43	16.0	2.98	0.69	7.41	12.3	5.97	27.1	0.01	96.38
KT 349B 4b 2	8.39	15.6	0.63	15.8	3.62	1.32	7.49	11.9	5.80	27.2	0.06	97.69
KT 349B 5a 1	0.01	8.69	0.00	20.1	9.87	0.00	11.4	12.6	6.44	27.4	0.18	96.70
KT349A 11 2	0.22	7.08	0.13	21.1	15.7	0.00	10.6	12.2	5.04	26.7	0.01	98.77
UK 298A 3c 5	0.00	1.76	0.00	71.7	0.09	0.00	2.99	1.18	3.57	20.5	0.00	101.77
others												
KT 349B 34b 1 *	0.02	0.62	0.00	5.70	0.11	0.14	29.5	22.5	0.00	32.4	0.27	91.26
KT 349B 34b 2 *	0.01	0.70	0.00	5.07	0.10	0.50	29.3	21.6	0.00	32.7	0.25	90.23
KT 344B 6 1 *	0.14	0.00	0.00	0.51	0.28	0.00	25.6	25.6	0.00	32.7	0.20	92.83
KT 349B 34b 3	0.05	0.30	0.00	0.14	0.12	0.00	73.1	0.23	0.00	26.7	0.06	100.70
KT 123 1 6	3.67	1.37	0.10	0.01	3.33	0.00	68.8	0.99	0.16	18.4	0.11	96.94

*: semiquantitative analysis.

"prassoite", $Rh_{17}S_{15}$, Pd–Hg (possibly potarite), Ir–Fe and Os–Fe alloys and an unknown Ir–Fe oxide (Table 3). The internal texture suggests that a primary interstitial complex grain of isoferroplatinum, and possibly erlichmanite, was partially replaced by tulameenite and the other PGM by reaction with a late fluid.

There is also evidence that late hydrothermal fluids circulating during or soon after fracturing of chromian spinel may have affected primary isoferroplatinum without resulting in a change in its composition. One polygonal grain with composition $Pt_{2.99}(Fe_{0.97}Ni_{0.02}Cu_{0.02})_{\Sigma 1.01}$ is located in chromite close to a large fracture filled with serpentine and Fe oxides (Fig. 9D, KT349D–22a). The alloy maintains sharp and straight contacts with fresh chromite, as is typical of primary inclusions, although minute apophyses having the form

TABLE 4 (continued). SELECTED RESULTS OF ELECTRON-MICROPROBE ANALYSES OF
PGM ASSOCIATED WITH Pt ALLOYS FROM CHROMITITES,
KYTLYM (KT) AND UKTUS (UK) COMPLEXES, RUSSIA

Grain No.	Os	Ir	Ru	Rh	Pt	Pd	Ni	Fe	Cu	S	As
Osmium											
KT 344C 34 1 at.%	87.7	3.46	0.65	0.35	5.16	0.15	1.86	0.67	0.00	0.00	0.00
KT 344D 12 3	93.0	1.51	0.59	0.46	2.91	0.09	0.52	0.92	0.00	0.00	0.00
KT 344D 1b 1	92.2	5.84	0.67	0.02	0.74	0.04	0.33	0.13	0.00	0.00	0.03
KT 344D 20 2	96.2	2.21	0.44	0.00	0.24	0.03	0.33	0.24	0.00	0.00	0.31
KT 344D 4a 1	87.5	6.21	0.76	0.83	2.92	0.13	0.61	0.93	0.00	0.00	0.11
KT344D 12 10	85.1	5.00	0.58	0.43	4.01	0.09	0.87	3.89	0.00	0.00	0.03
UK 296A 5b 2	96.0	1.26	0.34	0.23	1.93	0.00	0.14	0.07	0.00	0.00	0.03
Erlichmanite											
KT 349B 36a 3	27.5	2.03	3.76	0.58	0.17	0.09	0.12	0.19	0.04	65.4	0.12
KT 349C 13 2	22.5	1.90	5.47	1.43	0.00	0.27	0.04	0.47	0.12	67.8	0.00
KT 349C 13 3	21.1	2.37	7.00	1.54	0.00	0.24	0.19	0.56	0.30	66.7	0.00
UK 298A 3c 3	29.8	2.46	0.42	1.05	0.00	0.00	0.04	0.13	0.00	66.1	0.00
Cooperite											
KT 349B 45b 1	0.01	0.34	0.12	0.90	48.9	0.84	1.39	0.00	0.00	47.5	0.00
KT349A 13a 1	0.01	0.00	0.00	0.30	49.7	0.88	1.11	0.00	0.00	48.0	0.00
UK 298A 6 1	0.03	0.15	0.00	0.70	50.6	0.39	0.93	0.00	0.00	47.2	0.00
UK 298B 5 2	4.44	0.40	1.47	0.73	41.4	0.22	0.58	0.69	0.77	49.3	0.00
Rh–Ir–Pt thiospinels											
KT 349B 12a 2	0.48	5.91	0.00	18.9	3.01	1.35	4.11	7.41	7.33	51.5	0.00
KT 349B 2c 1	0.00	6.02	0.00	20.4	3.46	0.00	0.19	4.93	10.9	54.1	0.00
KT 349B 4b 3 *	0.98	6.60	0.32	10.7	9.56	0.14	0.89	3.81	10.4	56.6	0.00
KT 349C 5 3	0.84	12.4	0.07	12.5	4.26	0.50	0.08	4.01	8.76	56.5	0.08
KT 349A 16 4	1.01	5.72	0.12	20.0	5.57	0.00	0.12	6.75	5.60	55.1	0.01
UK 296A 12 1	0.09	11.6	0.00	17.7	0.35	0.00	1.19	0.62	10.2	58.2	0.05
UK 296A 3 1	0.00	6.90	0.00	9.04	13.1	0.00	0.05	0.41	13.0	57.5	0.00
UK 296A 3 2	0.00	6.76	0.00	9.34	13.2	0.31	0.00	0.47	13.3	56.6	0.02
UK 296A 4 1 *	0.03	8.10	0.00	7.82	13.5	0.00	0.16	0.09	12.8	57.5	0.00
unknown Rh–Ir sulfides											
KT 349B 2a 3	4.03	4.14	0.40	8.27	2.17	0.00	10.7	13.6	4.08	52.6	0.01
KT 349B 4b 1	2.81	4.90	0.27	9.79	0.96	0.41	7.94	13.8	5.91	53.2	0.01
KT 349B 4b 2	2.76	5.07	0.39	9.58	1.16	0.78	8.00	13.4	5.71	53.1	0.05
KT 349B 5a 1	0.00	2.72	0.00	11.7	3.04	0.00	11.6	13.6	6.09	51.1	0.15
KT349A 11 2	0.07	2.25	0.08	12.5	4.94	0.00	11.0	13.4	4.86	50.9	0.00
UK 298A 3c 5	0.00	0.62	0.00	47.3	0.03	0.00	3.44	1.43	3.78	43.4	0.00
others											
KT 349B 34b 1 *	0.00	0.16	0.00	2.78	0.03	0.07	25.4	20.3	0.00	51.1	0.16
KT 349B 34b 2 *	0.00	0.17	0.00	2.50	0.03	0.24	25.4	19.6	0.00	51.9	0.16
KT 344B 6 1 *	0.04	0.00	0.00	0.22	0.06	0.00	27.6	22.3	0.00	49.6	0.18
KT 349B 34b 3	0.01	0.08	0.00	0.06	0.03	0.00	59.7	0.19	0.00	39.9	0.03
KT 123 1 6	1.07	0.41	0.06	0.00	0.96	0.00	64.7	0.98	0.14	31.6	0.08

*: semiquantitative analysis.

of very small thorns appear to extend from the alloy grain into the chromian spinel along fissures. The texture possibly suggests that the apophyses may have grown by dissolution and redeposition of the same Pt alloy along the grain boundary, or by mechanical reworking during or soon after fracturing of chromian spinel, as also reported in studies of platinum nuggets (Cabri & Genkin 1991).

COMPARISON WITH PT ALLOYS
FROM ALLUVIAL NUGGETS OF THE URALS

A recent overview of the PGE mineralogy in alluvial placers of the Urals (Cabri *et al.* 1996, Makeyev *et al.* 1997) has confirmed previous results (Razin 1976) indicating the existence of two populations of nuggets: one, dominated by Pt–Fe alloys with subordinate Os–Ir
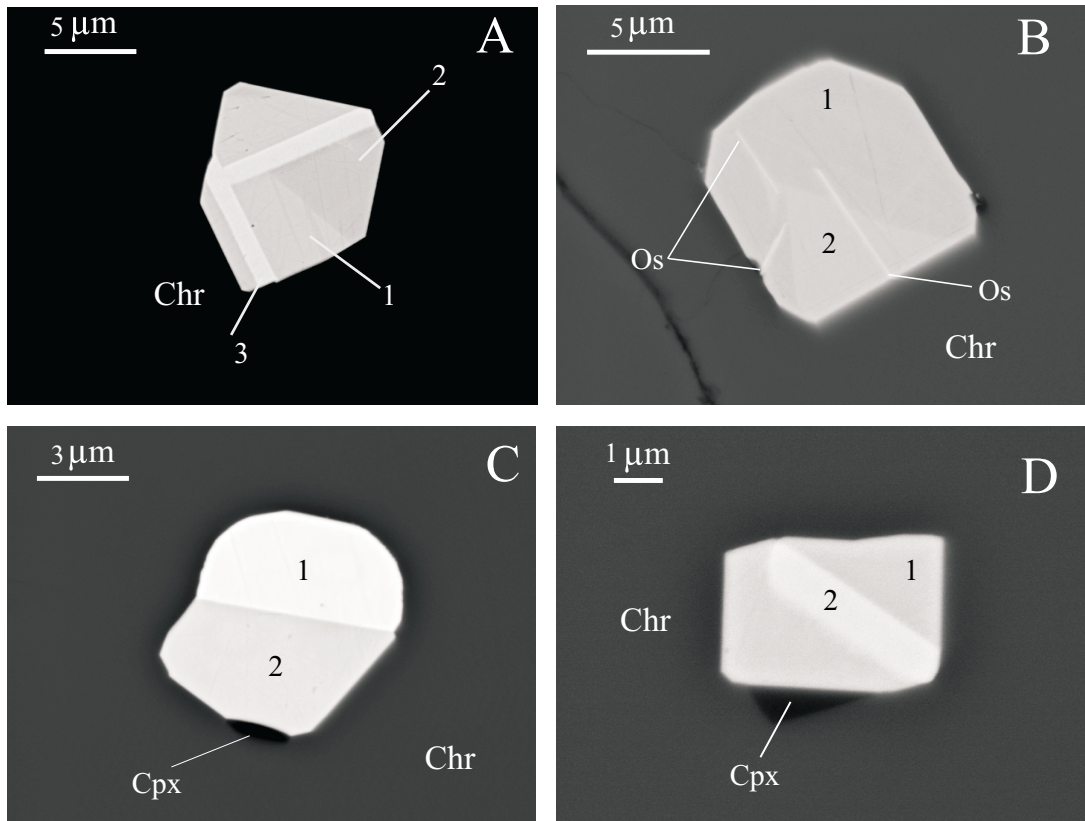
Fig. 7. BSE images of primary composite grains of Pt–Fe–Ni–(Cu) alloy included in chromian spinel (Chr) from the Kytlym chromitites. A) Grain KT344D–12, lamellar intergrowth possibly formed by subsolidus unmixing between Ni-rich isoferroplatinum $Pt_{2.54}(Fe_{1.2}Ni_{0.21}Cu_{0.05})_{\Sigma 1.46}$ (1), and tetraferroplatinum $Pt_{1.08}(Fe_{0.67}Ni_{0.17}Cu_{0.08})_{\Sigma 0.92}$ (2), associated with large exsolution-induced domains (?) of native osmium $Os_{0.98}Ir_{0.1}Ru_{0.1}$ (3). B) Grain KT344D–1a, coarse polygonal intergrowth of Ni-rich isoferroplatinum $Pt_{2.61}(Fe_{1.1}Ni_{0.23}Cu_{0.05})_{\Sigma 1.39}$ (1) and tetraferroplatinum $Pt_{1.1}(Fe_{0.625}Ni_{0.185}Cu_{0.09})_{\Sigma 0.9}$ (2) with minute exsolution-induced domain of native osmium (Os). C) Grain KT344D–20, compositionally homogeneous tetraferroplatinum $Pt_{1.08}(Fe_{0.63}Ni_{0.195}Cu_{0.095})_{\Sigma 0.92}$ (2) associated with native osmium $Os_{0.97}Ir_{0.02}Ru_{0.01}$, and clinopyroxene. D) Grain KT344D–4c, compositionally homogeneous tetraferroplatinm $Pt_{1.08}(Fe_{0.595}Ni_{0.225}Cu_{0.1})_{\Sigma 0.92}$ with exsolved (?) native osmium $Os_{0.93}Ir_{0.06}Ru_{0.01}$, associated with clinopyroxene.

alloys, is considered to have been derived from the erosion of Uralian–Alaskan zoned complexes; the other, mainly composed of Ru–Os alloys and laurite, is believed to have originated by the erosion of the ultramafic portion of ophiolite complexes. The two PGM assemblages can be found superimposed in one single placer deposit as a result of the coexistence of different rock associations in the same area, or caused by intricate processes of rewashing of ancient alluvial placers possibly derived from completely eroded complexes (Makeyev *et al.* 1997). The PGM nuggets from placer deposits of the Platinum-bearing Belt mainly consist of Pt–Fe alloys. At the locality Nizhni Tagil (Fig. 1B), the close similarity in mineral assemblage and texture observed between the placer nuggets and the lode PGM has been used to demonstrate that the nuggets were essentially a detrital product of the erosion of the upstream ultramafic bodies (dunite, chromitite), and did not form in a surficial environment (Cabri & Genkin 1991). Such a direct correlation could not be established in the case of Kytlym and Uktus, owing to the lack of information on placer deposits at these localities. However, comparison with the compositional data compiled by Cabri *et al.* (1996) for the Platinum-bearing Belt reveals a close similarity in the relative abundance of the Pt alloys (Fig. 11). The paragenetic relationships of the Pt alloys that we have observed in the chromitites of Kytlym and Uktus are practically the same as those

reported from the alluvial nuggets of the Urals (Cabri *et al.* 1996, Cabri & Genkin 1991, Genkin 1994): isoferroplatinum and tetraferroplatinum are primary phases, characteristically intergrown with accessory osmium, erlichmanite, cooperite, Rh–Ir–Pt thiospinels, and kashinite occurring as inclusions, exsolution-in-duced blebs, or small attached particles, whereas tulameenite is secondary, and typically replaces the pri-mary Pt alloys. The study of the chromitites of Kytlym and Uktus conclusively demonstrates that this PGM assemblage formed *in situ*, under a wide range of tem-peratures from early magmatic to hydrothermal, and, by analogy, supports the conclusion that the Pt-alloy nug-gets are detrital material derived from the erosion of Uralian–Alaskan-type complexes, and that the chromi-tites in these complexes are major contributors of the Pt alloys.

A major point that needs some discussion concerns the difference in grain size between the PGM inclusions in chromitites described in this work, and the alluvial nuggets reported from the Urals, which commonly range from 150 µm to 2 mm or more (Makeyev *et al.* 1997, Cabri *et al.* 1996). This difference has been frequently observed between lode and placer deposits in general, and has been used by some authors to question the de-trital nature of the nuggets. We believe that it may be an artifact produced by several concomitant factors. For example, most panning techniques fail to recover very small particles below the critical size of about 20–40 µm, such as those commonly visible by microscope on polished sections. Furthermore, both the size and tex-
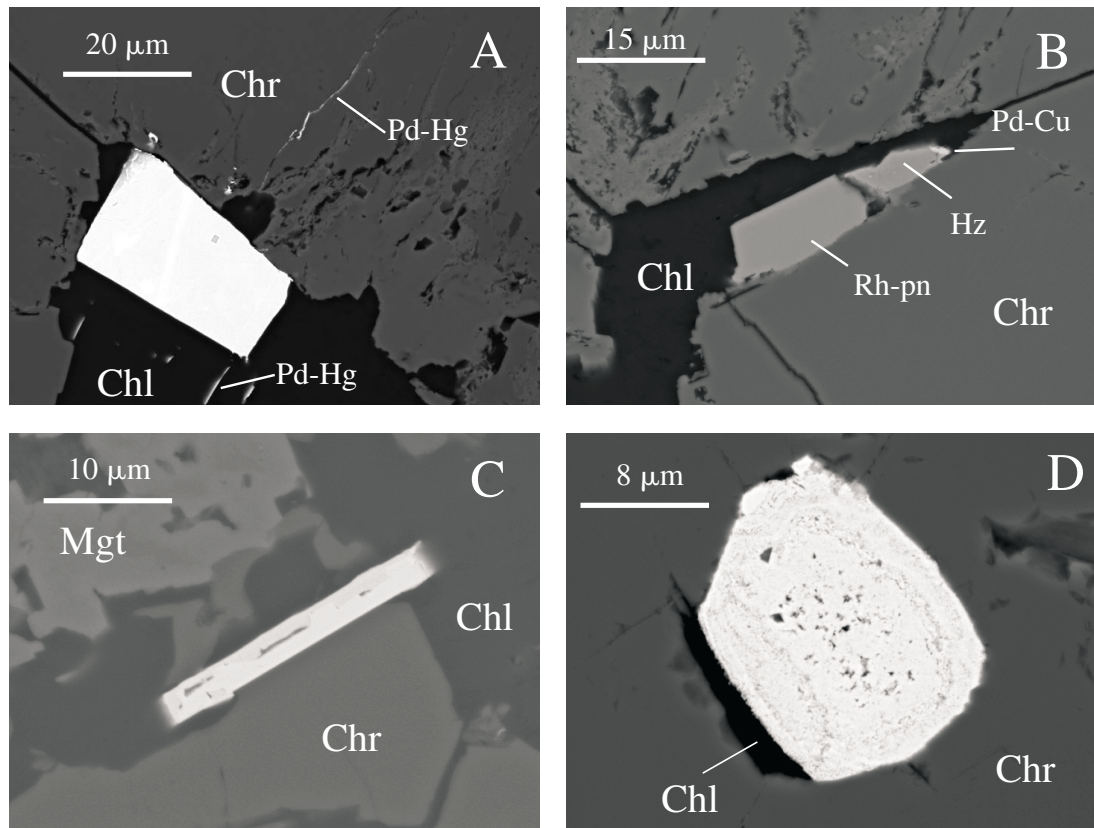
FIG. 8. BSE images of secondary Pt–Fe–Cu–(Ni) alloy from the Kytlym and Uktus chromitites. A) Grain KT349B–34a, tulameenite $Pt_{2.08}Fe_{0.94}(Cu_{0.93}Ni_{0.05})_{\Sigma 0.98}$ including a small crystal of irarsite (grey), occurs within chlorite (Chl) in contact with ferrian chromite (Chr). Fine veins of potarite (Pd–Hg) fill fractures in altered chromian spinel and cleavage planes in chlorite. B) Grain KT349B–34a, rhodian pentlandite (Rh–pn) $(Ni_{4.31}Fe_{3.31}Rh_{0.43})_{\Sigma 8.05}(S_{8.92}As_{0.03})_{\Sigma 8.95}$, heazlewoodite (Hz) and unknown Pd–Cu alloy hosted in chlorite (Chl) in contact with altered chromian spinel (Chr). C) Grain KT349D–27b 1, tulameenite including lamellae of Fe oxide, associated with magnetite (Mgt), ferrian chromite (Chr) and chlorite (Chl). D) Grain UK296A–9, porous tulameenite $Pt_{2.0}Fe_{1.11}(Cu_{0.76}Ni_{0.13})_{\Sigma 0.89}$ intergrown with an unidentified Cu-rich Pt alloy (grey coronas), associated with chlorite (Chl) and ferrian chromite (Chr).
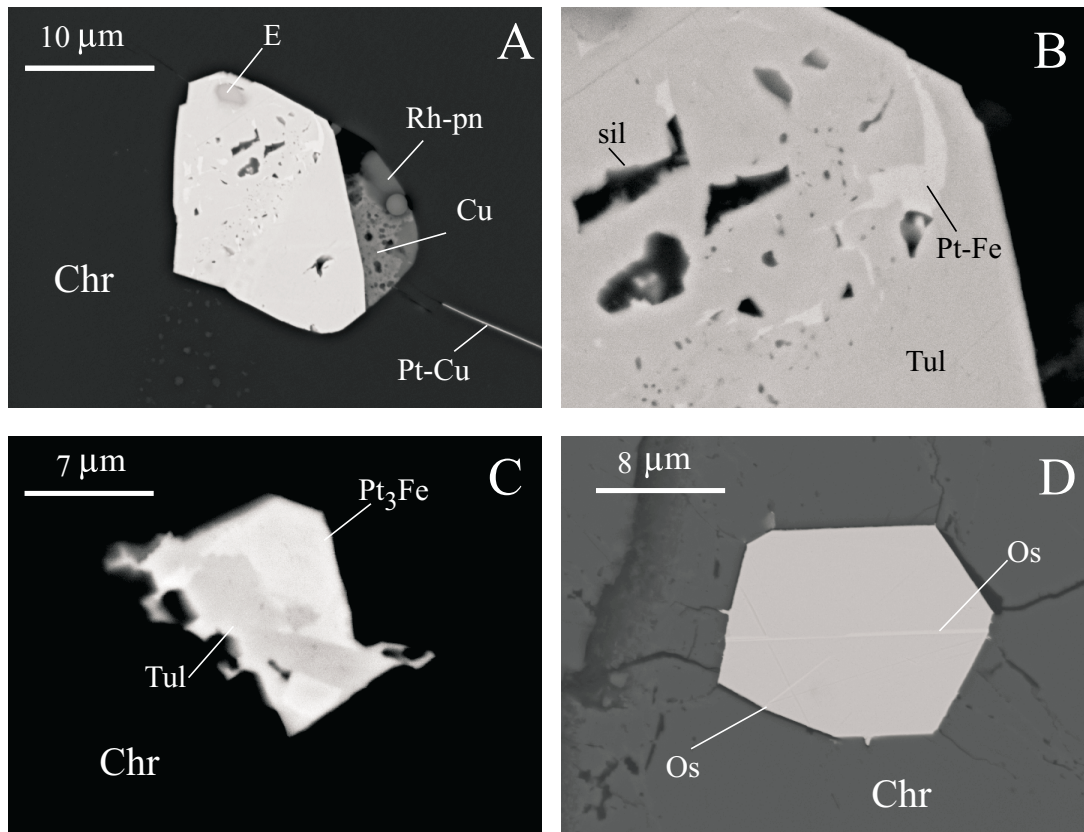
Fig. 9. BSE images of secondary Pt–Fe–Cu–(Ni) alloy from the Kytlym and Uktus chromitites. A) Grain KT349B–36a, tulameenite $Pt_{2.06}Fe_{1.21}(Ni_{0.05}Cu_{0.68})_{\Sigma0.73}$ associated with erlichmanite (E), rhodian pentlandite (Rh–pn) and native copper (Cu). Pt–Cu alloy occurs as fissure filling in chromian spinel (Chr). B) Enlargement of grain KT349B–36a showing signs of exsolution or relics (?) of a Pt–Fe alloy in porous tulameenite (Tul), pitted with silicate inclusions (sil). C) Grain UK296B–9, isoferroplatinum (Pt_3Fe) replaced by compositionally heterogeneous tulameenite (Tul) $Pt_{2.25-2.38}Fe_{0.92-0.96}$ $(Ni_{0.19-0.17}Cu_{0.64-0.49})_{\Sigma0.82-0.69}$ in altered chromite (Chr). D) Grain KT349D–22a, primary isoferroplatinum $Pt_{2.99}(Fe_{0.97}Ni_{0.02}$ $Cu_{0.02})_{\Sigma1.01}$ with fine exsolution-induced lamellae of osmium (Os), located in chromian spinel (Chr) close to a large fracture filled with serpentine and Fe oxides. Minute apophyses protrude from the alloy boundary into the chromian spinel along fissures and cracks, possibly indicating late mobilization.

tural position of the PGM in the source rocks may exert a major influence on their degree of liberation. Most grains of PGM that occur locked in chromite are in the size range of 1–35 μm, and are not expected to be liberated during mechanical disruption of the chromitites, but they more likely remain included in detrital chromite grains, thus escaping recovery by panning. PGM grains of a size comparable with the nuggets have been found located interstitially to chromite crystals (Fig. 10) or associated with interstitial silicates (Fig. 8A). Although extremely dispersed throughout the lode chromitites, these grains are probably more frequent than indicated by the study of polished sections, and therefore they represent the best candidates as the source material for the placer nuggets.

For these reasons, we consider the analogy in composition, relative abundance and paragenetic assemblage as the most conclusive factors establishing a genetic correlation between the Pt alloys in the chromitites of Uralian–Alaskan-type complexes and those in the alluvial nuggets of the Platinum-bearing Belt of the Urals.

Concluding Remarks

The Pt alloys associated with chromitites in the zoned complexes of Kytlym and Uktus are compositionally attributable to pure isoferroplatinum (Pt_3Fe), Ni-rich isoferroplatinum $Pt_{2.5}(Fe,Ni,Cu)_{\Sigma1.5}$ and tetraferroplatinum $Pt(Fe,Ni,Cu)$, ferronickelplatinum Pt_2FeNi, and tulameenite Pt_2FeCu. The alloys Pt_3Fe and
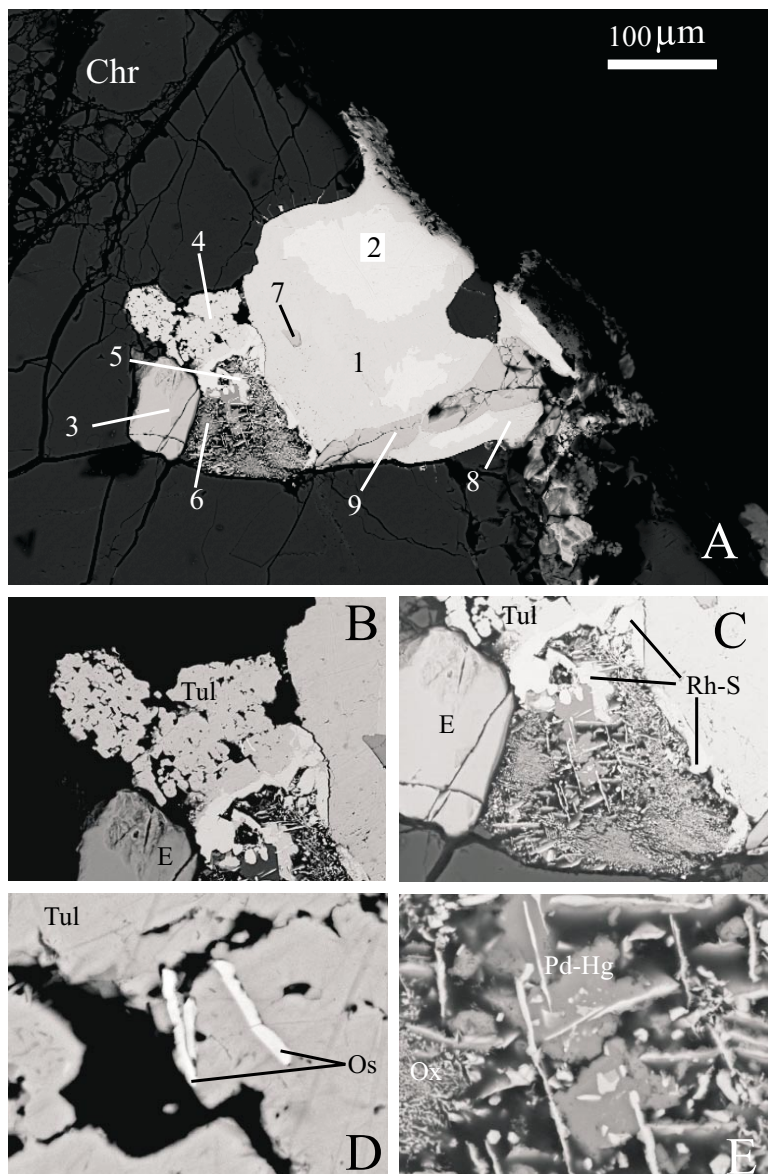
FIG. 10. BSE images of the largest PGM inclusion from the Uktus chromitites. A) Large-scale view of the grain (UK298A–3c), tulameenite, (1, and 8) $Pt_{2.07}Fe_{0.88}(Ni_{0.03}Cu_{1.02})_{\Sigma 1.05}$ replaces isoferroplatinum (2) $Pt_3(Fe_{0.97}Ni_{0.02}Cu_{0.01})_{\Sigma 1}$ along grain boundaries. Erlichmanite (E) occurs at the points 3, 7, and 9, with average composition $(Os_{0.89}Ir_{0.07}Rh_{0.03}Ru_{0.01})_{\Sigma 1}S_2$. (4) Sponge-like Ni-rich tulameenite (Tul) $Pt_{2.13}Fe_{1.26}(Ni_{0.15}Cu_{0.46})_{\Sigma 0.61}$ intergrown with chlorite (Chl) and containing lamellae of native osmium (Os) (see also enlarged fields B and D). (5) Unknown $(Rh_{15.1}Ir_{0.2}Ni_{1.1}Cu_{1.2}Fe_{0.5})_{\Sigma 18.1}S_{13.9}$, possibly prassoite (Rh–S), in contact with tulameenite (Tul) and erlichmanite (E) (see also enlarged fields B and C). (6) Complex intergrowth consisting of a matrix of minute Ir–Fe oxide (Ox) and Mg–Al silicate, containing probable potarite (Pd–Hg) associated with rods and hexagonal plates of Ir–Fe alloy (see also enlarged fields C and E).

the Ni-rich varieties $Pt_{2.5}(Fe,Ni,Cu)_{\Sigma1.5}$ and $Pt(Fe,Ni,Cu)$ precipitated at the highest temperatures in a pre-chromite stage, whereas members of the tulameenite series, characterized by high Cu contents, are believed to have crystallized after chromite, at a late stage, possibly from a hydrothermal solution.

As documented in studies of phase relations in the system Pt–Fe–S at high temperatures [Makovicky *et al.* (1986) and references therein], isoferroplatinum is the only Pt alloy phase stable in a sulfide-rich assemblage. The alloy formed at a high-temperature stage and was stable at $f(S_2)$ increasing up to, and exceeding the buffers Os–OsS$_2$, Pt–PtS and Fe–FeS, until it was captured during growth of chromian spinel together with the sulfides erlichmanite, cooperite and pyrrhotite. Electron-microprobe data indicate that isoferroplatinum crystallizing under these conditions has a composition very close to pure Pt_3Fe, possibly suggesting that the rise of $f(S_2)$ forced both Ni and Cu to enter the structure of coexisting sulfides. At low values of $f(S_2)$, the stable Pt alloys are Pt-deficient and incorporate variable amounts of Ni and, to a lesser extent, Cu, giving rise to a solid-solution series between $Pt_{2.5}(Fe,Ni,Cu)_{\Sigma1.5}$ and $Pt(Fe,Ni,Cu)$ in which Ni and Cu increase sympathetically, both substituting for Pt. The observation of an intergrowth of the two end members suggests that the solid solution is probably limited by some low-temperature miscibility gap.

Pure isoferroplatinum and the Ni-rich varieties of isoferroplatinum and tetraferroplatinum all contain lamellae of native osmium that may be interpreted to be the result of subsolidus exsolution. The relative abundance and the size of the lamellae indicate that much larger amounts of Os were incorporated in Ni-rich isoferroplatinum $Pt_{2.5}(Fe,Ni,Cu)_{\Sigma1.5}$ and Ni-rich tetraferroplatinum $Pt(Fe,Ni,Cu)$ compared with pure isoferroplatinum Pt_3Fe. This feature is ascribed to the fact that during deposition of Ni-rich Pt alloys, $f(S_2)$ was not sufficient for the reaction Os → OsS$_2$, leaving Os to enter freely the Pt alloy structure.

By analogy with other Uralian–Alaskan-type complexes (Nixon *et al.* 1990, Cabri & Genkin 1991), tulameenite encountered in chromitites of Kytlym and Uktus has the paragenetic characteristics of a late phase. Tulameenite occurs in an assemblage of secondary PGM and base metals enriched in Pd, Rh, Pt, and Cu, locally with secondary Ni sulfides and very rare Ir sulfarsenide. Some of the Pd, Pt, and Cu phases accompanying tulameenite are found as fissure fillings in chromite or form veins along the cleavage of chlorite, bearing witness to the late deposition of these metals by circulating hydrothermal solutions. Tulameenite found in replacement associations may have formed by chemical reaction of primary Pt alloys with Cu-rich fluids (Nixon *et al.* 1990), although it is possible that some large euhedral crystals of tulameenite isolated in interstitial patches of chlorite may have precipitated directly from a fluid phase at a relatively low temperature. In both cases, tulameenite shows variable values of Cu/Ni, which may be alternatively ascribed to incomplete replacement of the primary Pt alloy by tulameenite, or fluctuation in the activities of Cu and Ni in the hydrothermal fluid during precipitation of tulameenite.

A comparison of the present data with the extensive database on placer nuggets from the Urals provides further evidence that Pt alloy nuggets in placer deposits
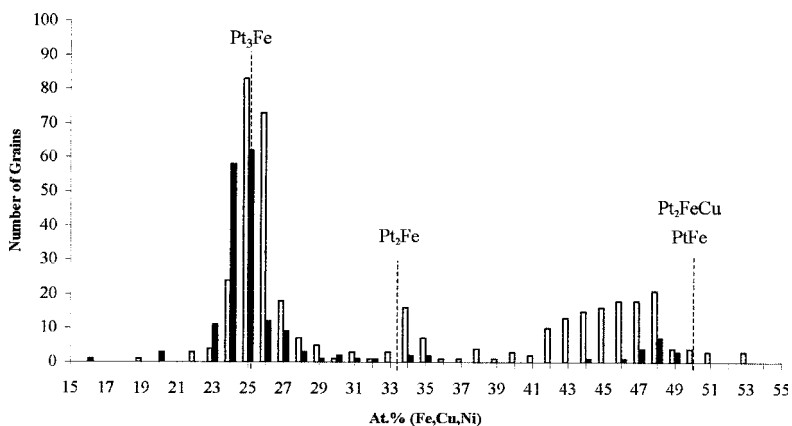

FIG. 11.   Frequency diagram showing the proportion of (Fe,Cu,Ni) in Pt alloys (at.%) from the Kytlym and Uktus chromitites (386 grains, white) and from placer nuggets of the Urals (183 grains, black). Theoretical stoichiometries of isoferroplatinum (Pt_3Fe), tulameenite (Pt_2FeCu), tetraferroplatinum (PtFe), and unnamed Pt_2Fe are shown for reference. Data for placer nuggets are taken from Tables B.1, B.3, and B.6 of Cabri *et al.* (1996).

may well be detrital in origin, and supports the working hypothesis that they were largely derived from the erosion of chromitites hosted in the dunite portions of Uralian–Alaskan-type complexes similar to those of Kytlym and Uktus.

REFERENCES

ANIKINA, E.V., PUSHKAREV, E.V., GARUTI, G., ZACCARINI, F. & SEDLER, I. (1999): Chrome-Platinum deposits in the Ural–Alaskan type complexes: composition and genesis. *In* Uralian Summer School of Mineralogy 1999: "Under the Platinum Sign" (Ekaterinburg), 62-82 (in Russ.).

BETEKHTIN, A.G. (1961): Mikroscopische Untersuchungen an Platinerzen aus dem Ural. *Neues Jahrb. Mineral., Abh.* **97**, 1-34.

CABRI, L.J., CRIDDLE, A.J., LAFLAMME, J.H.G., BEARNE, G.S. & HARRIS, D.C. (1981): Mineralogical study of complex Pt–Fe nuggets from Ethiopia. *Bull. Minéral.* **104**, 508-525.

_____ & FEATHER, C.E. (1975): Platinum–iron alloys: a nomenclature based on a study of natural and synthetic alloys. *Can. Mineral.* **13**, 117-126.

_____ & GENKIN, A.D. (1991): Re-examination of Pt alloys from lode and placer deposits, Urals. *Can. Mineral.* **29**, 419-425.

_____, HARRIS, D.C. & WEISER, T.W. (1996): Mineralogy and distribution of platinum-group mineral (PGM) placer deposits of the world. *Explor. Mining Geol.* **5**, 73-167.

_____, OWENS, D.R. & LAFLAMME, J.H.G. (1973): Tulameenite, a new platinum – iron – copper mineral from placers in the Tulameen river area, British Columbia. *Can. Mineral.* **12**, 21-25.

_____, ROSENSWEIG, A. & PINCH, W.W. (1977): Platinum group minerals from Onverwacht. 1. Pt–Fe–Cu–Ni alloys. *Can. Mineral.* **15**, 380-384.

DALTRY, V.D.C. & WILSON, A.H. (1997): Review of platinum-group mineralogy: compositions and elemental associations of the PG-minerals and unidentified PGE-phases. *Mineral. Petrol.* **60**, 185-229.

GARUTI, G., GAZZOTTI, M. & TORRES-RUIZ, J. (1995): Iridium, rhodium and platinum sulfides in chromitites from the ultramafic massifs of Finero, Italy, and Ojén, Spain. *Can. Mineral.* **33**, 509-520.

_____, ZACCARINI, F., CABELLA, R., ANIKINA, E. & PUSKAREV, E. (1996): Platinum-group minerals from the zoned ultramafic intrusion of Uktus (central Urals, Russia). *76° Convegno SIMP* (*Bologna*), *Riassunti. Plinius* **16**, 121-122.

GENKIN, A.D. (1994): Sequence and conditions of formation of platinum group minerals in Nizhni Tagil dunite massif. *Seventh Int. Platinum Symp.* (*Moscow*), 30-31 (abstr.).

MAKEYEV, A.B., KONONKOVA, N.N., KRAPLYA, E.A., CHERNUKHA, F.P. & BRYANCHANINOVA, N.I. (1997): Platinum group minerals in alluvium of the northern Urals and Timan: the key to primary sources of platinum. *Dokl. Russ. Acad. Sci., Earth Sci. Sect.* **353**, 181-184.

MAKOVICKY, M., MAKOVICKY, E. & ROSE-HANSEN, J. (1986): Experimental studies on the solubility and distribution of platinum group elements in base-metal sulphides in platinum deposits. *In* Metallogeny of Basic and Ultrabasic Rocks (M.J. Gallagher, R.A. Ixer, C.R. Neary & H.M. Prichard, eds.). Institute of Mining and Metallurgy, London, U.K. (415-425).

NIXON, G.T., CABRI, L.J. & LAFLAMME, J.H.G. (1990): Platinum-group-element mineralization in lode and placer deposits associated with the Tulameen Alaskan-type complex, British Columbia. *Can. Mineral.* **28**, 503-535.

PUSHKAREV, E.V. (2000): *Petrology of the Uktus Dunite – Clinopyroxenite – Gabbro Massif* (*Middle Urals*). The Russian Academy of Sciences, Ural Branch, Institute of Geology and Geochemistry, Ekaterinburg, Russia (in Russ.).

_____, ANIKINA, YE.V., GARUTI, G., ZACCARINI, F. & CABELLA, R. (1999): Geikielite (Mg-ilmenite) in association with Cr-spinel and platinoids from the Uktus massif dunites, Middle Urals: genetic implications. *Dokl. Earth Sci.* **369A**, 1220-1223.

_____, GULAYEVA, T.Y., PALGUEVA, G.V., PETRISHEVA, V.G. & SHERSTOBITOVA, D.A. (1994): The dunites of the Uktus massif. *In* Geology and Geochemistry, Ural Branch, Russ. Acad. Sci., Year Book 1993, Sverdlovsk, Russia (73-79, in Russ.).

_____ & PUCHKOVA, A.V. (1991): The Uktus mafic–ultramafic massif (middle Urals). *In* Geology and Geochemistry, Ural Branch, Russ. Acad. Sci., Year Book 1990, Sverdlovsk, Russia (35-37, in Russ.).

RAZIN, L.V. (1976): Geologic and genetic features of forsterite dunites and their platinum-group mineralization. *Econ. Geol.* **71**, 1371-1376.

RUDASHEVSKII, N.S., MOCHALOV, A.G., MEN'SHIKOV, YU.P. & SHUMSKAYA, N.I. (1983): Ferronickelplatinum Pt$_2$FeNi: a new mineral type. *Zap. Vses. Mineral. Obshchest.* **112**, 487-494 (in Russ.).

VOLCHENKO, Y.A., ZOLOEV, K.K., KOROTEEV, V.A. & MARDIROSIAN, A.N. (1995): The types of platinum deposits and their genetic essence. Actual problems of magmatic geology, petrology and ore formation. *In* Geology and Geochemistry, Ural Branch, Russ. Acad. Sci., Year Book 1995, Ekaterinburg, Russia (38-55, in Russ.).

YEFIMOV, A.A., YEFIMOVA, L.P. & MAEGOV, V.I. (1993): The tectonics of the platinum-bearing belt of the Urals: composition and mechanism of structural developments. *Geotectonics* **27**, 197-207.